

The No-Scale Multiverse at the LHC *

Tianjun Li,^{1,2} James A. Maxin,¹ Dimitri V. Nanopoulos,^{1,3,4} and Joel W. Walker⁵

¹*George P. and Cynthia W. Mitchell Institute for Fundamental Physics,
Texas A&M University, College Station, TX 77843, USA*

²*Key Laboratory of Frontiers in Theoretical Physics, Institute of Theoretical Physics,
Chinese Academy of Sciences, Beijing 100190, P. R. China*

³*Astroparticle Physics Group, Houston Advanced Research Center (HARC), Mitchell Campus, Woodlands, TX 77381, USA*

⁴*Academy of Athens, Division of Natural Sciences,
28 Panepistimiou Avenue, Athens 10679, Greece*

⁵*Department of Physics, Sam Houston State University, Huntsville, TX 77341, USA*

We present a contemporary perspective on the String Landscape and the Multiverse of plausible string, M- and F-theory vacua, seeking to demonstrate a non-zero probability for the existence of a universe matching our own observed physics within the solution ensemble. We argue for the importance of No-Scale Supergravity as an essential common underpinning for the spontaneous emergence of a cosmologically flat universe from the quantum “nothingness”. Our context is a highly detailed phenomenological probe of No-Scale \mathcal{F} - $SU(5)$, a model representing the intersection of the \mathcal{F} -lipped $SU(5) \times U(1)_X$ Grand Unified Theory (GUT) with extra TeV-Scale vector-like multiplets derived out of \mathcal{F} -theory, and the dynamics of No-Scale Supergravity. The latter in turn imply a very restricted set of high energy boundary conditions.

We present a highly constrained “Golden Point” located near $M_{1/2} = 455$ GeV and $\tan \beta = 15$ in the $\tan \beta - M_{1/2}$ plane, and a highly non-trivial “Golden Strip” with $\tan \beta \simeq 15$, $m_t = 173.0$ - 174.4 GeV, $M_{1/2} = 455$ - 481 GeV, and $M_V = 691$ - 1020 GeV, which simultaneously satisfies all the known experimental constraints, featuring also an imminently observable proton decay rate. We supplement this bottom-up phenomenological perspective with a top-down theoretical analysis of the one-loop effective Higgs potential. A striking consonance is achieved via the dynamic determination of $\tan \beta$ and $M_{1/2}$ for fixed Z -boson mass at the local *minimum minimorum* of the potential, that being the secondary minimization of the spontaneously broken electroweak Higgs vacuum V_{\min} . By also indirectly determining the electroweak scale, we suggest that this constitutes a complete resolution of the Standard Model gauge hierarchy problem.

Finally, we present the distinctive collider level signatures of No-Scale \mathcal{F} - $SU(5)$ for the $\sqrt{s} = 7$ TeV LHC, with 1 fb^{-1} of integrated luminosity. The characteristic feature is a light stop and gluino, both sparticles lighter than all other squarks, generating a surplus of ultra-high multiplicity (≥ 9) hadronic jet events. We propose modest alterations to the canonical background selection cut strategy which are expected to yield significantly enhanced resolution of the characteristic ultra-high jet multiplicity \mathcal{F} - $SU(5)$ events, while readily suppressing the contribution of all Standard Model processes, and allowing moreover a clear differentiation from competing models of new physics, most notably minimal supergravity. Detection by the LHC of the ultra-high jet signal would constitute a suggestive evocation of the intimately linked stringy origins of \mathcal{F} - $SU(5)$, and could provide a glimpse into the underlying structure of the fundamental string moduli, possibly even opening a darkened glass upon the hidden workings of the No-Scale Multiverse.

PACS numbers: 11.10.Kk, 11.25.Mj, 11.25.-w, 12.60.Jv

I. INTRODUCTION

The number of consistent, meta-stable vacua of string, M- or (predominantly) F-theory flux compactifications which exhibit broadly plausible phenomenology, including moduli stabilization and broken supersymmetry [1–6], is popularly estimated [7, 8] to be of order 10^{500} . It is moreover currently in vogue to suggest that degeneracy of common features across these many “universes”

might statistically isolate the physically realistic universe from the vast “landscape”, much as the entropy function coaxes the singular order of macroscopic thermodynamics from the chaotic duplicity of the entangled quantum microstate. We argue here though the counter point that we are not obliged *a priori* to live in the likeliest of all universes, but only in one which is possible. The existence merely of a non-zero probability for our existence is sufficient.

We indulge for this effort the fanciful imagination that the “Multiverse” of string vacua might exhibit some literal realization beyond our own physical sphere. A single electron may be said to wander all histories through interfering apertures, though its arrival is ultimately registered at a localized point on the target. The journey to that destination is steered by the full dynamics of the

* Submitted to the Fifth International Workshop DICE 2010: Space, Time, Matter - Current Issues in Quantum Mechanics and Beyond, September 13-17, 2010, Castello Pasquini, Italy, based on the invited talk by D.V.N.

theory, although the isolated spontaneous solution reflects only faintly the richness of the solution ensemble. Whether the Multiverse be reverie or reality, the conceptual superset of our own physics which it embodies must certainly represent the interference of all navigable universal histories.

Surely many times afore has mankind's notion of the heavens expanded - the Earth dispatched from its central pedestal in our solar system and the Sun rendered one among some hundred billion stars of the Milky Way, itself reduced to one among some hundred billion galaxies. Finally perhaps, we come to the completion of our Odyssey, by realizing that our Universe is one of at least 10^{500} so possible, thus rendering the anthropic view of our position in the Universe (environmental coincidences explained away by the availability of $10^{11} \times 10^{11}$ solar systems) functionally equivalent to the anthropic view of the origin of the Universe (coincidences in the form and content of physical laws explained away by the availability, through dynamical phase transitions, of 10^{500} universes). Nature's bounty has anyway invariably trumped our wildest anticipations, and though frugal and equanimous in law, she has spared no extravagance or whimsy in its manifestation.

Our perspective should not be misconstrued, however, as complacent retreat into the tautology of the weak anthropic principle. It is indeed unassailable truism that an observed universe must afford and sustain the life of the observer, including requisite constraints, for example, on the cosmological constant [9] and gauge hierarchy. Our point of view, though, is sharply different; We should be able to resolve the cosmological constant and gauge hierarchy problems through investigation of the fundamental laws of our (or any single) Universe, its accidental and specific properties notwithstanding, without resorting to the existence of observers. In our view, the observer is the output of, not the *raison d'être* of, our Universe. Thus, our attention is advance from this base camp of our own physics, as unlikely an appointment as it may be, to the summit goal of the master theory and symmetries which govern all possible universes. In so seeking, our first halting forage must be that of a concrete string model which can describe Nature locally.

II. THE ENSEMBLE MULTIVERSE

The greatest mystery of Nature is the origin of the Universe itself. Modern cosmology is relatively clear regarding the occurrence of a hot big bang, and subsequent Planck, grand unification, cosmic inflation, lepto- and baryogenesis, and electroweak epochs, followed by nucleosynthesis, radiation decoupling, and large scale structure formation. In particular, cosmic inflation can address the flatness and monopole problems, explain homogeneity, and generate the fractional anisotropy of the cosmic background radiation by quantum fluctuation of the inflaton field [10–14]. A key question though, is from

whence the energy of the Universe arose. Interestingly, the gravitational field in an inflationary scenario can supply the required positive mass-kinetic energy, since its potential energy becomes negative without bound, allowing that the total energy could be exactly zero.

Perhaps the most striking revelation of the post-WMAP [15–17] era is the decisive determination that our Universe is indeed globally flat, *i.e.*, with the net energy contributions from baryonic matter $\simeq 4\%$, dark matter $\simeq 23\%$, and the cosmological constant (dark energy) $\simeq 73\%$ finely balanced against the gravitational potential. Not long ago, it was possible to imagine the Universe, with all of its physics intact, hosting any arbitrary mass-energy density, such that “ $k = +1$ ” would represent a super-critical cosmology of positive curvature, and “ $k = -1$ ” the sub-critical case of negative curvature. In hindsight, this may come to seem as naïve as the notion of an empty infinite Cartesian space. The observed energy balance is highly suggestive of a fundamental symmetry which protects the “ $k = 0$ ” critical solution, such that the physical constants of our Universe may not be divorced from its net content.

This null energy condition licenses the speculative connection *ex nihilo* of our present universe back to the primordial quantum fluctuation of an external system. Indeed, there is nothing which quantum mechanics abhors more than nothingness. This being the case, an extra universe here or there might rightly be considered no extra trouble at all! Specifically, it has been suggested [10–12, 18, 19] that the fluctuations of a dynamically evolved expanding universe might spontaneously produce tunneling from a false vacuum into an adjacent (likely also false) meta-stable vacuum of lower energy, driving a local inflationary phase, much as a crystal of ice or a bubble of steam may nucleate and expand in a super-cooled or super-heated fluid during first order transition. In this “eternal inflation” scenario, such patches of space will volumetrically dominate by virtue of their exponential expansion, recursively generating an infinite fractal array of causally disconnected “Russian doll” universes, nesting each within another, and each featuring its own unique physical parameters and physical laws.

From just the specific location on the solution “target” where our own Universe landed, it may be impossible to directly reconstruct the full theory. Fundamentally, it may be impossible even in principle to specify why our particular Universe is precisely as it is. However, superstring theory and its generalizations may yet present to us a loftier prize - the theory of the ensemble Multiverse.

III. THE INVARIANCE OF FLATNESS

More important than any differences between various possible vacua are the properties which might be invariant, protected by basic symmetries of the underlying mechanics. We suppose that one such basic property must be cosmological flatness, so that the seedling uni-

verse may transition dynamically across the boundary of its own creation, maintaining a zero balance of some suitably defined energy function. In practice, this implies that gravity must be ubiquitous, its negative potential energy allowing for positive mass and kinetic energy. Within such a universe, quantum fluctuations may not again cause isolated material objects to spring into existence, as their net energy must necessarily be positive. For the example of a particle with mass m on the surface of the Earth, the ratio of gravitational to mass energy is more than nine orders of magnitude too small

$$\left| -\frac{G_N M_E m}{R_E} \right| \div mc^2 \simeq 7 \times 10^{-10}, \quad (1)$$

where G_N is the gravitational constant, c is the speed of light, and M_E and R_E are the mass and radius of the Earth, respectively. Even in the limiting case of a Schwarzschild black hole of mass M_{BH} , a particle of mass m at the horizon $R_S = 2G_N M_{BH}/c^2$ has a gravitational potential which is only half of that required.

$$\left| -\frac{G_N M_{BH} m}{R_S} \right| = \frac{1}{2} mc^2 \quad (2)$$

It is important to note that while the energy density for the gravitational field is surely negative in Newtonian mechanics, the global gravitational field energy is not well defined in general relativity. Unique prescriptions for a stress-energy-momentum pseudotensor can be formulated though, notably that of Landau and Lifshitz. Any such stress-energy can, however, be made to vanish locally by general coordinate transformation, and it is not even entirely clear that the pseudotensor so applied is an appropriate general relativistic object. Given though that Newtonian gravity is the classical limit of general relativity, it is reasonable to suspect that the properly defined field energy density will be likewise also negative, and that inflation is indeed consistent with a correctly generalized notion of constant, zero total energy.

A universe would then be in this sense closed, an island unto itself, from the moment of its inception from the quantum froth; Only a universe *in toto* might so originate, emerging as a critically bound structure possessing profound density and minute proportion, each as accorded against intrinsically defined scales (the analogous Newton and Planck parameters and the propagation speed of massless fields), and expanding or inflating henceforth and eternally.

IV. THE INVARIANCE OF NO-SCALE SUGRA

Inflation, driven by the scalar inflaton field is itself inherently a quantum field theoretic subject. However, there is tension between quantum mechanics and general relativity. Currently, superstring theory is the best candidate for quantum gravity. The five consistent ten dimensional superstring theories, namely heterotic $E_8 \times E_8$, het-

erotic $SO(32)$, Type I, Type IIA, Type IIB, can be unified by various duality transformations under an eleven-dimensional M-theory [20], and the twelve-dimensional F-theory can be considered as the strongly coupled formulation of the Type IIB string theory with a varying axion-dilaton field [21]. Self consistency of the string (or M-, F-) algebra implies a ten (or eleven, twelve) dimensional master spacetime, some elements of which – six (or seven, eight) to match our observed four large dimensions – may be compactified on a manifold (typically Calabi-Yau manifolds or G_2 manifolds) which conserves a requisite portion of supersymmetric charges.

The structure of the curvature within the extra dimensions dictates in no small measure the particular phenomenology of the unfolded dimensions, secreting away the “closet space” to encode the symmetries of all gauged interactions. The physical volume of the internal spatial manifold is directly related to the effective Planck scale and basic gauge coupling strengths in the external space. The compactification is in turn described by fundamental moduli fields which must be stabilized, *i.e.*, given suitable vacuum expectation values (VEVs).

The famous example of Kaluza and Klein prototypes the manner in which general covariance in five dimensions is transformed to gravity plus Maxwell theory in four dimensions when the transverse fifth dimension is cycled around a circle. The connection of geometry to particle physics is perhaps nowhere more intuitively clear than in the context of model building with $D6$ -branes, where the gauge structure and family replication are related directly to the brane stacking and intersection multiplicities. The Yukawa couplings and Higgs structure are in like manners also specified, leading after radiative symmetry breaking of the chiral gauge sector to low energy masses for the chiral fermions and broken gauge generators, each massless in the symmetric limit.

From a top-down view, Supergravity (SUGRA) is an ubiquitous infrared limit of string theory, and forms the starting point of any two-dimensional world sheet or D-dimensional target space action. The mandatory localization of the Supersymmetry (SUSY) algebra, and thus the momentum-energy (space-time translation) operators, leads to general coordinate invariance of the action and an Einstein field theory limit. Any available flavor of Supergravity will not however suffice. In general, extraneous fine tuning is required to avoid a cosmological constant which scales like a dimensionally suitable power of the Planck mass. Neglecting even the question of whether such a universe might be permitted to appear spontaneously, it would then be doomed to curl upon itself and collapse within the order of the Planck time, for comparison about 10^{-43} seconds in our Universe. Expansion and inflation appear to uniquely require properties which arise naturally only in the No-Scale SUGRA formulation [22–26].

SUSY is in this case broken while the vacuum energy density vanishes automatically at tree level due to a suitable choice of the Kähler potential, the function which

specifies the metric on superspace. At the minimum of the null scalar potential, there are flat directions which leave the compactification moduli VEVs undetermined by the classical equations of motion. We thus receive without additional effort an answer to the deep question of how these moduli are stabilized; They have been transformed into dynamical variables which are to be determined by minimizing corrections to the scalar potential at loop order. In particular, the high energy gravitino mass $M_{3/2}$, and also the proportionally equivalent universal gaugino mass $M_{1/2}$, will be established in this way. Subsequently, all gauge mediated SUSY breaking soft-terms will be dynamically evolved down from this boundary under the renormalization group [27], establishing in large measure the low energy phenomenology, and solving also the Flavour Changing Neutral Current (FCNC) problem. Since the moduli are fixed at a false local minimum, phase transitions by quantum tunneling will naturally occur between discrete vacua.

The specific Kähler potential which we favor has been independently derived in both weakly coupled heterotic string theory [28] and the leading order compactification of M-theory on S^1/Z_2 [29], and might be realized in F-theory models as well [30–33]. We conjecture, for the reasons given prior, that the No-Scale SUGRA construction could pervade all universes in the String Landscape with reasonable flux vacua. This being the case, intelligent creatures elsewhere in the Multiverse, though separated from us by a bridge too far, might reasonably so concur after parallel examination of their own physics. Moreover, they might leverage via this insight a deeper knowledge of the underlying Multiverse-invariant master theory, of which our known string, M-, and F-theories may compose some coherently overlapping patch of the garment edge. Perhaps we yet share appreciation, across the cords which bind our 13.7 billion years to their corresponding blink of history, for the common timeless principles under which we are but two isolated condensations upon two particular vacuum solutions among the physical ensemble.

V. AN ARCHETYPE MODEL UNIVERSE

Though we engage in this work lofty and speculative questions of natural philosophy, we balance abstraction against the measured material underpinnings of concrete phenomenological models with direct and specific connection to tested and testable particle physics. If the suggestion is correct that eternal inflation and No-Scale SUGRA models with string origins together describe what is in fact our Multiverse, then we must as a prerequisite settle the issue of whether our own phenomenology can be produced out of such a construction.

In the context of Type II intersecting D-brane models, we have indeed found one realistic Pati-Salam model which might describe Nature as we observe it [34–36]. If only the F-terms of three complex structure moduli are

non-zero, we also automatically have vanishing vacuum energy, and obtain a generalized No-Scale SUGRA. It seems to us that the string derived Grand Unified Theories (GUTs), and particularly the Flipped $SU(5) \times U(1)_X$ models [37–39], are also candidate realistic string models with promising predictions that can be tested at the Large Hadron Collider (LHC), the Tevatron, and other future experiments.

Let us briefly review the minimal flipped $SU(5) \times U(1)_X$ model [37–39]. The gauge group of the flipped $SU(5)$ model is $SU(5) \times U(1)_X$, which can be embedded into $SO(10)$. We define the generator $U(1)_{Y'}$ in $SU(5)$ as

$$T_{U(1)_{Y'}} = \text{diag} \left(-\frac{1}{3}, -\frac{1}{3}, -\frac{1}{3}, \frac{1}{2}, \frac{1}{2} \right). \quad (3)$$

The hypercharge is given by

$$Q_Y = \frac{1}{5} (Q_X - Q_{Y'}). \quad (4)$$

In addition, there are three families of SM fermions whose quantum numbers under the $SU(5) \times U(1)_X$ gauge group are

$$F_i = (\mathbf{10}, \mathbf{1}), \quad \bar{f}_i = (\bar{\mathbf{5}}, -\mathbf{3}), \quad \bar{l}_i = (\mathbf{1}, \mathbf{5}), \quad (5)$$

where $i = 1, 2, 3$.

To break the GUT and electroweak gauge symmetries, we introduce two pairs of Higgs fields

$$H = (\mathbf{10}, \mathbf{1}), \quad \bar{H} = (\bar{\mathbf{10}}, -\mathbf{1}), \\ h = (\mathbf{5}, -\mathbf{2}), \quad \bar{h} = (\bar{\mathbf{5}}, \mathbf{2}). \quad (6)$$

Interestingly, we can naturally solve the doublet-triplet splitting problem via the missing partner mechanism [39], and then the dimension five proton decay from the colored Higgsino exchange can be highly suppressed [39]. The flipped $SU(5) \times U(1)_X$ models have been constructed systematically in the free fermionic string constructions at Kac-Moody level one previously [39–43], and in the F-theory model building recently [30–33, 44, 45].

In the flipped $SU(5) \times U(1)_X$ models, there are two unification scales: the $SU(3)_C \times SU(2)_L$ unification scale M_{32} and the $SU(5) \times U(1)_X$ unification scale $M_{\mathcal{F}}$. To separate the M_{32} and $M_{\mathcal{F}}$ scales and obtain true string-scale gauge coupling unification in free fermionic string models [43, 46] or the decoupling scenario in F-theory models [44, 45], we introduce vector-like particles which form complete flipped $SU(5) \times U(1)_X$ multiplets. In order to avoid the Landau pole problem for the strong coupling constant, we can only introduce the following two sets of vector-like particles around the TeV scale [46]

$$Z1 : XF = (\mathbf{10}, \mathbf{1}), \quad \bar{X}\bar{F} = (\bar{\mathbf{10}}, -\mathbf{1}); \quad (7)$$

$$Z2 : XF, \bar{X}\bar{F}, Xl = (\mathbf{1}, -\mathbf{5}), \quad \bar{X}\bar{l} = (\mathbf{1}, \mathbf{5}), \quad (8)$$

where

$$XF \equiv (XQ, XD^c, XN^c), \quad \bar{X}\bar{l}_{(\mathbf{1}, \mathbf{5})} \equiv XE^c. \quad (9)$$

In the prior, XQ , XD^c , XE^c , XN^c have the same quantum numbers as the quark doublet, the right-handed down-type quark, charged lepton, and neutrino, respectively. Such kind of the models have been constructed systematically in the F-theory model building locally and dubbed $\mathcal{F} - SU(5)$ within that context [44, 45]. In this paper, we only consider the flipped $SU(5) \times U(1)_X$ models with Z2 set of vector-like particles. The discussions for the models with Z1 set and heavy threshold corrections [44, 45] are similar.

These models are moreover quite interesting from a phenomenological point of view [44, 45]. The predicted vector-like particles can be observed at the Large Hadron Collider, and the partial lifetime for proton decay in the leading $(e|\mu)^+\pi^0$ channels falls around 5×10^{34} years, testable at the future Hyper-Kamiokande [47] and Deep Underground Science and Engineering Laboratory (DUSEL) [48] experiments [49–51]. The lightest CP-even Higgs boson mass can be increased [52], hybrid inflation can be naturally realized, and the correct cosmic primordial density fluctuations can be generated [53].

VI. NO-SCALE SUPERGRAVITY

In the traditional framework, supersymmetry is broken in the hidden sector, and then its breaking effects are mediated to the observable sector via gravity or gauge interactions. In GUTs with gravity mediated supersymmetry breaking, also known as the minimal supergravity (mSUGRA) model, the supersymmetry breaking soft terms can be parameterized by four universal parameters: the gaugino mass $M_{1/2}$, scalar mass M_0 , trilinear soft term A , and the ratio of Higgs VEVs $\tan\beta$ at low energy, plus the sign of the Higgs bilinear mass term μ . The μ term and its bilinear soft term B_μ are determined by the Z-boson mass M_Z and $\tan\beta$ after the electroweak (EW) symmetry breaking.

To solve the cosmological constant problem, No-Scale supergravity was proposed [22–26]. No-scale supergravity is defined as the subset of supergravity models which satisfy the following three constraints [22–26]: (i) The vacuum energy vanishes automatically due to the suitable Kähler potential; (ii) At the minimum of the scalar potential, there are flat directions which leave the gravitino mass $M_{3/2}$ undetermined; (iii) The super-trace quantity $\text{Str}\mathcal{M}^2$ is zero at the minimum. Without this, the large one-loop corrections would force $M_{3/2}$ to be either zero or of Planck scale. A simple Kähler potential which satisfies the first two conditions is

$$K = -3\ln(T + \bar{T} - \sum_i \bar{\Phi}_i \Phi_i), \quad (10)$$

where T is a modulus field and Φ_i are matter fields. The third condition is model dependent and can always be satisfied in principle [54].

The scalar fields in the above Kähler potential parameterize the coset space $SU(N_C+1, 1)/(SU(N_C+1) \times U(1))$,

where N_C is the number of matter fields. Analogous structures appear in the $N \geq 5$ extended supergravity theories [55], for example, $N_C = 4$ for $N = 5$, which can be realized in the compactifications of string theory [28, 29]. The non-compact structure of the symmetry implies that the potential is not only constant but actually identical to zero. In fact, one can easily check that the scalar potential is automatically positive semi-definite, and has a flat direction along the T field. Interestingly, for the simple Kähler potential in Equation (10) we obtain the simplest No-Scale boundary condition $M_0 = A = B_\mu = 0$, while $M_{1/2}$ may be non-zero at the unification scale, allowing for low energy SUSY breaking.

It is important to note that there exist several methods of generalizing No-Scale supergravity, for instance, the previously mentioned Type II intersecting D-brane models [34–36], and the compactifications of M-theory on S^1/Z_2 with next-to-leading order corrections, where we have obtained a generalization employing modulus dominated SUSY breaking [56–60]. Similarly, mirage mediation for the flux compactifications can be considered as another form of generalized No-Scale supergravity [61, 62]. In this paper we concentrate on the simplest No-Scale supergravity, reserving any such generalizations for future study.

VII. THE GOLDEN POINT

First, we would like to review the Golden Point of No-Scale and no-parameter $\mathcal{F} - SU(5)$ [63]. In the No-Scale context, we impose $M_0 = A = B_\mu = 0$ at the unification scale $M_{\mathcal{F}}$, and allow distinct inputs for the single parameter $M_{1/2}(M_{\mathcal{F}})$ to translate under the RGEs to distinct low scale outputs of B_μ and the Higgs mass-squares $M_{H_u}^2$ and $M_{H_d}^2$. This continues until the point of spontaneous breakdown of the electroweak symmetry at $M_{H_u}^2 + \mu^2 = 0$, at which point minimization of the broken potential establishes the physical low energy values of μ and $\tan\beta$. In practice however, this procedure is at odds with the existing `SuSpect 2.34` code [64] base from which our primary routines have been adapted. In order to impose the minimal possible refactoring, we have instead opted for an inversion wherein $M_{1/2}$ and $\tan\beta$ float as two effective degrees of freedom. Thus, we do not fix $B_\mu(M_{\mathcal{F}})$. We take $\mu > 0$ as suggested by the results of $g_\mu - 2$ for the muon, and assume as in prior work that the masses for the vector-like particles are universal at 1 TeV.

The relic LSP neutralino density, WIMP-nucleon direct detection cross sections and photon-photon annihilation cross sections are computed with `MicrOMEGAs 2.1` [65] wherein the revised `SuSpect` RGEs have also implemented. We use a top quark mass of $m_t = 173.1$ GeV [66] and employ the following experimental constraints: (1) The WMAP 7-year measurements of the cold dark matter density [15–17], $0.1088 \leq \Omega_\chi \leq 0.1158$.

We allow Ω_χ to be larger than the upper bound due to a possible $\mathcal{O}(10)$ dilution factor [67] and to be smaller than the lower bound due to multicomponent dark matter. (2) The experimental limits on the FCNC process, $b \rightarrow s\gamma$. We use the limits $2.86 \times 10^{-4} \leq Br(b \rightarrow s\gamma) \leq 4.18 \times 10^{-4}$ [68, 69]. (3) The anomalous magnetic moment of the muon, $g_\mu - 2$. We use the 2σ level boundaries, $11 \times 10^{-10} < \Delta a_\mu < 44 \times 10^{-10}$ [70]. (4) The process $B_s^0 \rightarrow \mu^+\mu^-$ where we take the upper bound to be $Br(B_s^0 \rightarrow \mu^+\mu^-) < 5.8 \times 10^{-8}$ [71]. (5) The LEP limit on the lightest CP-even Higgs boson mass, $m_h \geq 114$ GeV [72, 73].

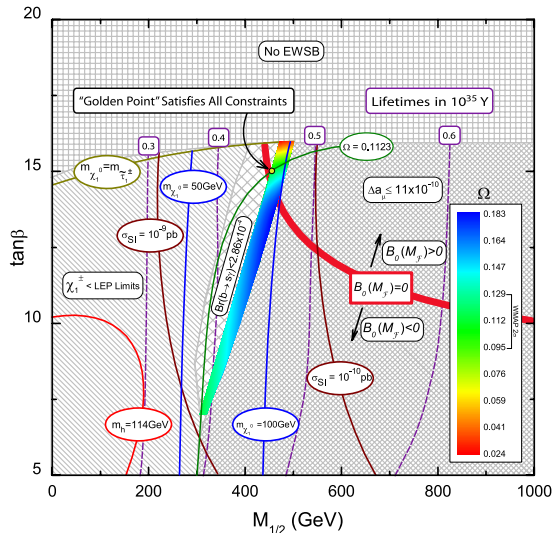


FIG. 1: Viable parameter space in the $\tan\beta - M_{1/2}$ plane. The “Golden Point” is annotated. The thin, dark green line denotes the WMAP 7-year central value $\Omega_\chi = 0.1123$. The dashed purple contours label $p \rightarrow (e|\mu)^+\pi^0$ proton lifetime predictions, in units of 10^{35} years.

In the $\tan\beta - M_{1/2}$ plane, $B_\mu(M_F)$ is then calculated along with the low energy supersymmetric particle spectrum and checks on various experimental constraints. The subspace corresponding to a No-Scale model is clearly then a one dimensional slice of this manifold, as demonstrated in Figure 1. It is quite remarkable that the $B_\mu(M_F) = 0$ contour so established runs sufficiently perpendicular to the WMAP strip that the point of intersection effectively absorbs our final degree of freedom, creating what we have labeled as a No-Parameter Model. It is truly extraordinary however that this intersection occurs exactly at the centrally preferred relic density, that being our strongest experimental constraint. We emphasize again that there did not have to be an experimentally viable $B_\mu(M_F) = 0$ solution, and that the consistent realization of this scenario depended crucially on several uniquely identifying characteristics of the underlying proposal. Specifically again, it appears that the No-Scale condition comes into its own only when applied at near the Planck mass, and that this is naturally identified as the point of the final \mathcal{F} - $SU(5)$ unification, which is

naturally extended and decoupled from the primary GUT scale only via the modification to the RGEs from the TeV scale \mathcal{F} -theory vector-like multiplet content. The union of our top-down model based constraints with the bottom-up experimental data exhausts the available freedom of parameterization in a uniquely consistent and predictive manner, phenomenologically defining a truly Golden Point near $M_{1/2} = 455$ GeV and $\tan\beta = 15$ GeV.

TABLE I: Spectrum (in GeV) for the Golden Point of Figure 1. Here, $\Omega_\chi = 0.1123$, $\sigma_{SI} = 1.9 \times 10^{-10}$ pb, and $\langle\sigma v\rangle_{\gamma\gamma} = 1.7 \times 10^{-28}$ cm^3/s . The central prediction for the $p \rightarrow (e|\mu)^+\pi^0$ proton lifetime is 4.6×10^{34} years.

$\tilde{\chi}_1^0$	95	$\tilde{\chi}_1^\pm$	185	\tilde{e}_R	150	\tilde{t}_1	489	\tilde{u}_R	951	m_h	120.1
$\tilde{\chi}_2^0$	185	$\tilde{\chi}_2^\pm$	826	\tilde{e}_L	507	\tilde{t}_2	909	\tilde{u}_L	1036	$m_{A,H}$	920
$\tilde{\chi}_3^0$	821	$\tilde{\nu}_{e/\mu}$	501	$\tilde{\tau}_1$	104	\tilde{b}_1	859	\tilde{d}_R	992	m_{H^\pm}	925
$\tilde{\chi}_4^0$	824	$\tilde{\nu}_\tau$	493	$\tilde{\tau}_2$	501	\tilde{b}_2	967	\tilde{d}_L	1039	\tilde{g}	620

Our Golden point features $M_{1/2} = 455.3$ GeV, $\tan\beta = 15.02$, and is in full compliance with the WMAP 7-year results, with $\Omega_\chi = 0.1123$. It also satisfies the CDMS II [74], Xenon 100 [75], and FERMI-LAT space telescope constraints [76], with $\sigma_{SI} = 1.9 \times 10^{-10}$ pb and $\langle\sigma v\rangle_{\gamma\gamma} = 1.7 \times 10^{-28}$ cm^3/s . The proton lifetime is about 4.6×10^{34} years, which is well within reach of the upcoming Hyper-Kamiokande [47] and DUSEL [48] experiments. Inspecting the supersymmetric particle and Higgs spectrum for the Golden Point of Table I reveals that the additional contribution of the 1 TeV vector-like particles lowers the gluino mass quite dramatically. The gluino mass M_3 runs flat from the M_{32} unification scale to 1 TeV as shown in Figure 2, though, due to supersymmetric radiative corrections, the physical gluino mass at the EW scale is larger than M_3 at the M_{32} scale. This is true for the full parameter space. For our data point, the LSP neutralino is 99.8% Bino. Similarly to the mSUGRA picture, our this point is in the stau-neutralino coannihilation region, but the gluino is lighter than the squarks in our models.

We plot gauge coupling and gaugino mass unification for the Golden Point in Figure 2. The figure explicitly demonstrates the two-step unification of flipped $SU(5) \times U(1)_X$. In addition, we present the RGE running for the μ term, the SUSY breaking scalar masses, trilinear A-terms, and bilinear B_μ term in Figure 3. Note in particular that the EW symmetry breaking occurs when $H_u^2 + \mu^2$ goes negative.

VIII. THE GOLDEN STRIP

Second, we shall review the Golden Strip of correlated top quark, gaugino, and vectorlike mass in No-Scale, no-parameter \mathcal{F} - $SU(5)$ [77]. From the above discussions, only a small portion of viable parameter space is consistent with the $B_\mu(M_F) = 0$ condition, which thus constitutes a strong constraint. Since the boundary value of

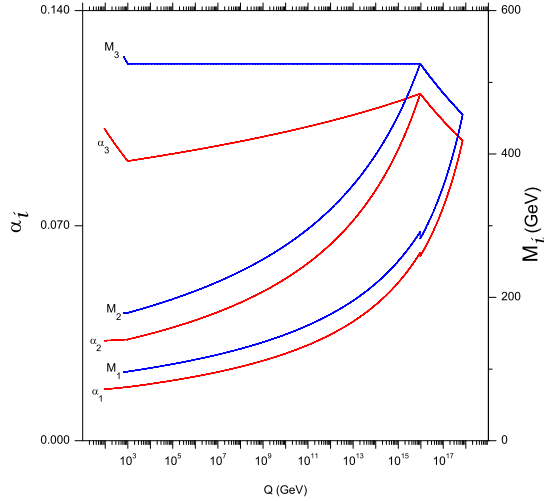


FIG. 2: RGE Running of the SM gauge couplings and gaugino masses from the EW scale to the unification scale $M_{\mathcal{F}}$. There is a discontinuity in the running at M_{32} due to remixing of the hypercharge with the residual Abelian phase from the breaking of $SU(5)$

the universal gaugino mass $M_{1/2}$, and even the unification scale $M_{\mathcal{F}} \simeq 7.5 \times 10^{17}$ GeV itself, are established by the low energy experiments via RGE running, we are not left with any surviving scale parameters in the present model. The floor of the “valley gorge” in Figure 4 represents accord with the $B_\mu = 0$ target for variations in $(M_{1/2}, M_V)$. We fix $\tan \beta = 15$, as appears to be rather generically required in No-Scale \mathcal{F} - $SU(5)$ to realize radiative EWSB and match the observed CDM density.

We have allowed for uncertainty in the most sensitive experimental input, the top quark mass, by effectively redefining m_t as an independent free parameter. Lesser sensitivities to uncertainty in (α_s, M_Z) are included in the ± 1 GeV deviation from strict adherence to $B_\mu = 0$. We have established that there is a two dimensional sheet (of some marginal thickness to recognize the mentioned uncertainty) defining $|B_\mu(M_{\mathcal{F}})| \leq 1$ for each point in the three dimensional $(M_{1/2}, M_V, m_t)$ volume, as shown in Figures (5,6). This sheet is inclined in the region of interest at the very shallow angle of 0.2° to the $(M_{1/2}, M_V)$ plane, such that m_t is largely decoupled from variation in the plane.

The $(g-2)_\mu$ and $b \rightarrow s\gamma$ constraints vary most strongly with $M_{1/2}$. The two considered effects are each at their lower limits at the boundary, but they exert pressure in opposing directions on $M_{1/2}$ due to the fact that the leading gaugino and squark contributions to $Br(b \rightarrow s\gamma)$ enter with an opposing sign to the SM term and Higgs contribution. For the non-SM contribution to Δa_μ , the effect is additive, and establishes an upper mass limit on $M_{1/2}$. Incidentally, the same experiment forms the central rationale for the adoption of $\text{sign}(\mu) > 0$, such that appropriate interference terms between SM and SUSY

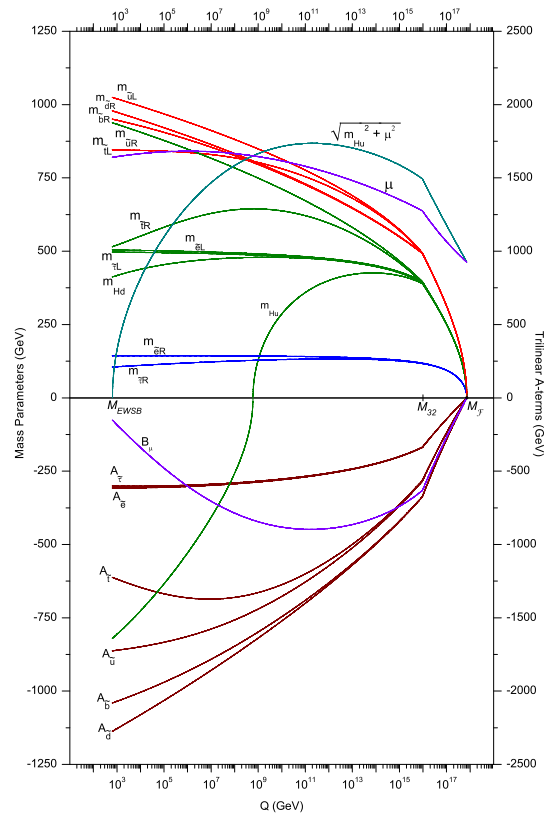


FIG. 3: RGE Running of the μ term and SUSY breaking soft terms from the EW scale to the unification scale $M_{\mathcal{F}}$.

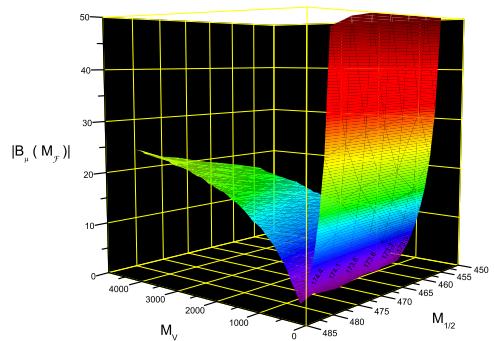


FIG. 4: The $B_\mu = 0$ target for variations in $(M_{1/2}, M_V)$, with $\tan \beta = 15$. The specific m_t which is required to minimize $|B_\mu(M_{\mathcal{F}})|$ is annotated along the solution string.

contributions are realized. Conversely, the requirement that SUSY contributions to $Br(b \rightarrow s\gamma)$ not be overly large, undoing the SM effect, requires a sufficiently large, *i.e.* lower bounded, $M_{1/2}$. The WMAP-7 CDM measurement, by contrast, exhibits a fairly strong correlation with both $(M_{1/2}, M_V)$, cross-cutting the $M_{1/2}$ bound, and confining the vectorlike mass to 691-1020 GeV. We note that the mixing of the SM fermions and vector par-

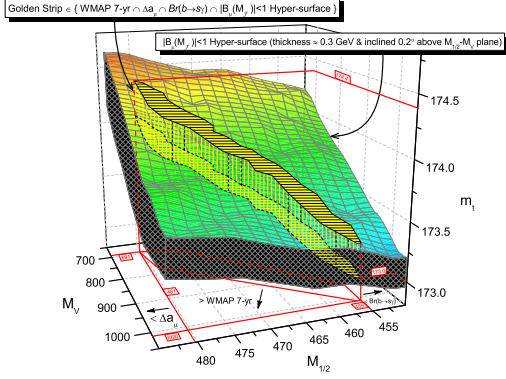


FIG. 5: With $\tan \beta \simeq 15$ fixed by WMAP-7, the residual parameter volume is three dimensional in $(M_{1/2}, M_V, m_t)$, with the $|B_\mu(M_F)| \leq 1$ (slightly thickened) surface forming a shallow (0.2°) incline above the $(M_{1/2}, M_V)$ plane.

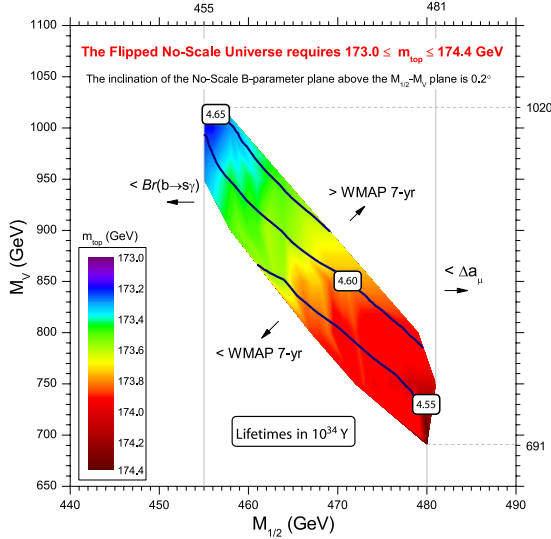


FIG. 6: A flattened presentation of the the $(M_{1/2}, M_V)$ plane depicted in Figure 5. The overlaid blue contours mark the $p \rightarrow (e|\mu)^+\pi^0$ proton lifetime prediction, in units of 10^{34} years.

ticles may give additional contributions to $Br(b \rightarrow s\gamma)$ and Δa_μ , but we do not consider them here.

The intersection of these three key constraints with the $|B_\mu(M_F)| \leq 1$ surface, as depicted in Figures (5,6), defines the “Golden Strip” of No-Scale \mathcal{F} - $SU(5)$. All of the prior is accomplished with no reference to the experimental top quark mass, redefined here as a *free* input. However, the extremely shallow angle of inclination (0.2°) of the $|B_\mu(M_F)| \leq 1$ sheet above the $(M_{1/2}, M_V)$ plane and into the m_t axis causes the Golden Strip to *imply* an exceedingly narrow range of compatibility for m_t , between 173.0-174.4 GeV, in perfect alignment with the physically observed value of $m_t = 173.1 \pm 1.3$ GeV [66].

Within the Golden Strip, we select the benchmark point of Table II. The Golden Strip is further consistent

with the CDMS II [74] and Xenon 100 [75] upper limits, with the spin-independent cross section extending from $\sigma_{SI} = 1.3\text{--}1.9 \times 10^{-10}$ pb. Likewise, the allowed region satisfies the Fermi-LAT space telescope constraints [76], with the photon-photon annihilation cross section $\langle\sigma v\rangle_{\gamma\gamma}$ ranging from $\langle\sigma v\rangle_{\gamma\gamma} = 1.5\text{--}1.7 \times 10^{-28} \text{ cm}^3/\text{s}$.

TABLE II: Spectrum (in GeV) for the benchmark point. Here, $M_{1/2} = 464$ GeV, $M_V = 850$ GeV, $m_t = 173.6$ GeV, $\Omega_\chi = 0.112$, $\sigma_{SI} = 1.7 \times 10^{-10}$ pb, and $\langle\sigma v\rangle_{\gamma\gamma} = 1.7 \times 10^{-28} \text{ cm}^3/\text{s}$. The central prediction for the $p \rightarrow (e|\mu)^+\pi^0$ proton lifetime is 4.6×10^{34} years. The lightest neutralino is 99.8% Bino.

$\tilde{\chi}_1^0$	96	$\tilde{\chi}_1^\pm$	187	\tilde{e}_R	153	\tilde{t}_1	499	\tilde{u}_R	975	m_h	120.6
$\tilde{\chi}_2^0$	187	$\tilde{\chi}_2^\pm$	849	\tilde{e}_L	519	\tilde{t}_2	929	\tilde{u}_L	1062	$m_{A,H}$	946
$\tilde{\chi}_3^0$	845	$\tilde{\nu}_{e/\mu}$	513	$\tilde{\tau}_1$	105	\tilde{b}_1	880	\tilde{d}_R	1018	m_{H^\pm}	948
$\tilde{\chi}_4^0$	848	$\tilde{\nu}_\tau$	506	$\tilde{\tau}_2$	514	\tilde{b}_2	992	\tilde{d}_L	1065	\tilde{g}	629

IX. THE SUPER NO-SCALE MECHANISM

In the following sections, we would like to review our study on Super No-Scale \mathcal{F} - $SU(5)$ [78, 79]. The single relevant modulus field in the simplest string No-Scale supergravity is the Kähler modulus T , a characteristic of the Calabi-Yau manifold, the dilaton coupling being irrelevant. The F-term of T generates the gravitino mass $M_{3/2}$, which is proportionally equivalent to $M_{1/2}$. Exploiting the simplest No-Scale boundary condition at M_F and running from high energy to low energy under the RGEs, there can be a secondary minimization, or *minimum minimorum*, of the minimum of the Higgs potential V_{\min} for the EWSB vacuum. Since V_{\min} depends on $M_{1/2}$, the gaugino mass $M_{1/2}$ is consequently dynamically determined by the equation $dV_{\min}/dM_{1/2} = 0$, aptly referred to as the “Super No-Scale” mechanism [78, 79].

It could easily have been that in consideration of the above technique, there were: A) too few undetermined parameters, with the $B_\mu = 0$ condition forming an incompatible over-constraint, and thus demonstrably false, or B) so many undetermined parameters that the dynamic determination possessed many distinct solutions, or was so far separated from experiment that it could not possibly be demonstrated to be true. The actual state of affairs is much more propitious, being specifically as follows. The three parameters M_0, A, B_μ are once again identically zero at the boundary because of the defining Kähler potential, and are thus known at all other scales as well by the RGEs. The minimization of the Higgs scalar potential with respect to the neutral elements of both SUSY Higgs doublets gives two conditions, the first of which fixes the magnitude of μ . The second condition, which would traditionally be used to fix B_μ , instead here enforces a consistency relationship on the remaining parameters, being that B_μ is already constrained.

In general, the $B_\mu = 0$ condition gives a hypersurface of solutions cut out from a very large parameter space. If we lock all but one parameter, it will give the final value. If we take a slice of two dimensional space, as has been described, it will give a relation between two parameters for all others fixed. In a three-dimensional view with B_μ on the vertical axis, this curve is the “flat direction” line along the bottom of the trench of $B_\mu = 0$ solutions. In general, we must vary at least two parameters rather than just one in isolation, in order that their mutual compensation may transport the solution along this curve. The most natural first choice is in some sense the pair of prominent unknown inputs $M_{1/2}$ and $\tan\beta$, as was demonstrated in Ref. [78, 79].

Having come to this point, it is by no means guaranteed that the potential will form a stable minimum. It must be emphasized that the $B_\mu = 0$ No-Scale boundary condition is the central agent affording this determination, as it is the extraction of the parameterized parabolic curve of solutions in the two compensating variables which allows for a localized, bound nadir point to be isolated by the Super No-Scale condition, dynamically determining *both* parameters. The background surface of V_{\min} for the full parameter space outside the viable $B_\mu = 0$ subset is, in contrast, a steadily inclined and uninteresting function. Although we have remarked that $M_{1/2}$ and $\tan\beta$ have no *directly* established experimental values, they are severely indirectly constrained by phenomenology in the context of this model [63, 77]. It is highly non-trivial that there should be accord between the top-down and bottom-up perspectives, but this is indeed precisely what has been observed [78, 79].

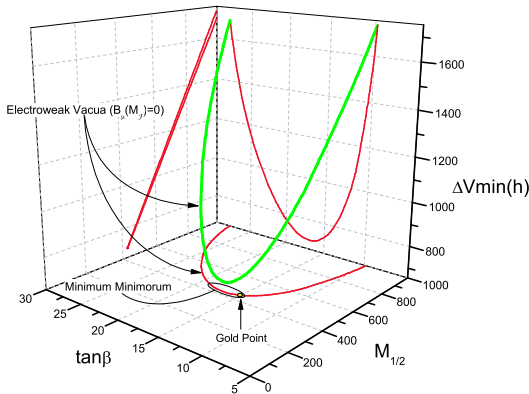


FIG. 7: The *minimum* V_{\min} of the Higgs effective potential (green curve, GeV) is plotted as a function of $M_{1/2}$ (GeV) and $\tan\beta$, emphasizing proximity of the “Golden Point” of Ref. [63] to the dynamic region of the V_{\min} *minimorum*.

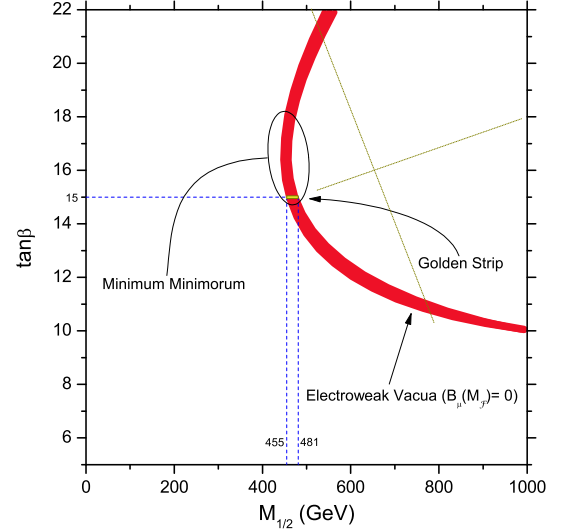


FIG. 8: The projection onto the $(M_{1/2}, \tan\beta)$ plane of Figure 7 is further detailed, expanding to span the boundary cases of the Ref. [77] “Golden Strip”. The symmetry axis of the $B_\mu = 0$ parabola is rotated slightly above the $M_{1/2}$ axis.

X. THE MINIMUM MINIMORUM OF THE HIGGS POTENTIAL: FIXING M_Z

We employ an effective Higgs potential in the ’t Hooft-Landau gauge and the $\overline{\text{DR}}$ scheme, given summing the following neutral tree (V_0) and one loop (V_1) terms.

$$\begin{aligned} V_0 &= (\mu^2 + m_{H_u}^2)(H_u^0)^2 + (\mu^2 + m_{H_d}^2)(H_d^0)^2 \\ &\quad - 2\mu B_\mu H_u^0 H_d^0 + \frac{g_2^2 + g_Y^2}{8} [(H_u^0)^2 - (H_d^0)^2]^2 \\ V_1 &= \sum_i \frac{n_i}{64\pi^2} m_i^4(\phi) \left(\ln \frac{m_i^2(\phi)}{Q^2} - \frac{3}{2} \right) \end{aligned} \quad (11)$$

Above, $m_{H_u}^2$ and $m_{H_d}^2$ are the SUSY breaking soft masses of the Higgs fields H_u and H_d , g_2 and g_Y are the gauge couplings of $SU(2)_L$ and $U(1)_Y$, n_i and $m_i^2(\phi)$ are the degree of freedom and mass for ϕ_i , and Q is the renormalization scale. We include the complete Minimal Supersymmetric Standard Model (MSSM) contributions to one loop, following Ref. [80], although the result is phenomenologically identical accounting only the leading top and partner stop terms. Since the minimum of the electroweak (EW) Higgs potential V_{\min} depends implicitly on $M_{3/2}$, the gravitino mass is determined by $dV_{\min}/dM_{3/2} = 0$. Being that $M_{1/2}$ is proportional to $M_{3/2}$, it is equivalent to employ $M_{1/2}$ directly as our modulus parameter, from which all other SUSY breaking soft terms here derive. In our numerical results in the figures, we shall designate differences in the fourth-root of the effective Higgs potential as $\Delta V_{\min}(h) \equiv V_{\text{eff}}^{1/4}$, measured in units of GeV relative to an arbitrary overall zero-offset.

Factors explicit within the potential are obtained from

our customized extension of the `SuSpect 2.34` [64] code-base, including a self-consistency assessment [63] on $B_\mu = 0$. We apply two-loop RGE running for the SM gauge couplings, and one-loop running for the SM fermion Yukawa couplings, μ term and soft terms.

Studying V_{\min} generically in the $(M_{1/2}, \tan\beta)$ plane, no point of secondary minimization is readily apparent in the strong, roughly linear, downward trend with respect to $M_{1/2}$ over the region of interest. However, the majority of the plane is not in physical communication with our model, disrespecting the fundamental $B_\mu = 0$ condition. Isolating only the compliant contour within this surface, *mirabile dictu*, a parabola is traced with nadir alighting gentle upon our original Golden Point, as in Figure (7). Restoring parameterization freedom to (M_V, m_t) , we may scan across the corresponding Golden Point of each nearby universe variant, reconstructing in their union the previously advertised Golden Strip, as in Figure (8). Notably, the theoretical restriction on $\tan\beta$ remains stable against variation in these parameters, exactly as its experimental counterpart. We find it quite extraordinary that the phenomenologically preferred region rests precisely at the curve’s locus of symmetric inflection. Note in particular that it is the selection of the parabolic $B_\mu = 0$ contour out of the otherwise uninteresting $V_{\min}(M_{1/2}, \tan\beta)$ inclined surface which allows a clear *minimum minimorum* to be established. We reiterate that consistency of the dynamically positioned $M_{1/2}$ and $\tan\beta$ with the Golden Strip, implies consistency with all current experimental data.

A strongly linear relationship is observed between the SUSY and EWSB scales with $M_{\text{EWSB}} \simeq 1.44 M_{1/2}$, such that a corresponding parabolic curve may be visualized. There is a charged stau LSP for $\tan\beta$ from 16 to 22, and we connect points with correct EWSB smoothly on the plot in this region. If $\tan\beta$ is larger than 22, the stau is moreover tachyonic, so properly we must restrict all analysis to $\tan\beta \leq 22$.

XI. THE GAUGE HIERARCHY PROBLEM

Not only must we explain stabilization of the electroweak scale against quantum corrections, but we must also explain why the electroweak scale and TeV-sized SUSY breaking soft-terms are “initially” positioned so far below the Planck mass. These latter components of the “gauge hierarchy” problem are the more subtle. In their theoretical pursuit, we do not though feign ignorance of established experimental boundaries, taking the phenomenologist’s perspective that pieces fit already to the puzzle stipulate a partial contour of those yet to be placed. Indeed, careful knowledge of precision electroweak scale physics, including the strong and electromagnetic couplings, the Weinberg angle and the Z-mass are required even to run the one loop RGEs. In the second loop one requires also *minimally* the leading top quark Yukawa coupling, as deduced from m_t , and the

Higgs VEV $v \equiv \sqrt{\langle H_u \rangle^2 + \langle H_d \rangle^2} \simeq 174$ GeV, established in turn from measurement of the effective Fermi coupling, or from M_Z and the electroweak couplings.

Reading the RGEs up from M_Z , we take unification of the gauge couplings as evidence of a GUT. Reading them in reverse from a point of high energy unification, we take the heaviness of the top quark, via its large Yukawa coupling, to dynamically drive the term $M_{H_u}^2 + \mu^2$ negative, triggering spontaneous collapse of the tachyonic vacuum, *i.e.* radiative electroweak symmetry breaking. Minimization of this potential with respect to the neutral components of H_u and H_d yields two conditions, which may be solved for $\mu(M_Z)$ and $B_\mu(M_Z)$ in terms of the constrained Higgs VEVs, which are in turn functions of M_Z (considered experimentally fixed) and $\tan\beta \equiv \langle H_u \rangle / \langle H_d \rangle$ (considered a free parameter).

Restricting to just the solution subset for which $B_\mu(M_Z)$ given by EWSB stitches cleanly onto that run down under the RGEs from $B_\mu(M_{\mathcal{F}}) = 0$, $\tan\beta$, or equivalently μ , becomes an implicit function of the single moduli $M_{1/2}(M_{\mathcal{F}})$. The pinnacle of this construction is the Super No-Scale condition $dV_{\min}/dM_{1/2} = 0$, wherein $M_{1/2}$, and thus also $\tan\beta$, are dynamically established at the local *minimum minimorum*. By comparison, the standard MSSM construction seems a hoax, requiring horrendous fine tuning to stabilize if viewed as a low energy supergravity limit, and moreover achieving TeV scale EW and SUSY physics as a simple shell game by manual selection of TeV scale boundaries for the soft terms $M_{1/2}$, M_0 , and A .

Strictly speaking, having effectively exchanged input of the Z-mass for a constraint on $\mu(M_{\mathcal{F}})$, we dynamically establish the SUSY breaking soft term $M_{1/2}$ and $\tan\beta$ *within* the electroweak symmetry breaking vacua, *i.e.* with fixed $v \simeq 174$ GeV. However, having predicted $M_{\mathcal{F}}$ as an output scale near the reduced Planck mass, we are licensed to invert the solution, taking $M_{\mathcal{F}}$ as a high scale *input* and dynamically addressing the gauge hierarchy through the standard story of radiative electroweak symmetry breaking. This proximity to the elemental high scale of (consistently decoupled) gravitational physics, arises because of the dual flipped unification and the perturbing effect of the TeV multiplets, and is not motivated in standard GUTs. Operating the machinery of the RGEs in reverse, we may transmute the low scale M_Z for the high scale $M_{\mathcal{F}}$, emphasizing that the fundamental dynamic *correlation* is that of the *ratio* $M_Z/M_{\mathcal{F}}$, taking either as our input yardstick according to taste. For fixed $M_{\mathcal{F}} \simeq 7 \times 10^{17}$ GeV, in a single breath we receive the order of the electroweak scale, the Z-mass, the Higgs bilinear coupling μ , the Higgs VEVs, and all other dependent dimensional quantities, including predictions for the full superparticle mass spectrum. It is in this sense that we claim a complete resolution of the gauge hierarchy problem, within the context of the Super No-Scale \mathcal{F} - $SU(5)$ model.

XII. THE GUT HIGGS MODULUS

An alternate pair of parameters for which one may attempt to isolate a $B_\mu = 0$ curve, which we consider for the first time in this work, is that of $M_{1/2}$ and the GUT scale M_{32} , at which the $SU(3)_C$ and $SU(2)_L$ couplings initially meet. Fundamentally, the latter corresponds to the modulus which sets the total magnitude of the GUT Higgs field's VEVs. M_{32} could of course in some sense be considered a “known” quantity, taking the low energy couplings as input. Indeed, starting from the measured SM gauge couplings and fermion Yukawa couplings at the standard 91.187 GeV electroweak scale, we may calculate both M_{32} and the final unification scale M_F , and subsequently the unified gauge coupling and SM fermion Yukawa couplings at M_F , via running of the RGEs. However, since the VEVs of the GUT Higgs fields H and \bar{H} are considered here as free parameters, the GUT scale M_{32} must not be fixed either. As a consequence, the low energy SM gauge couplings, and in particular the $SU(2)_L$ gauge coupling g_2 , will also run freely via this feedback from M_{32} .

We consider this conceptual release of a known quantity, in order to establish the nature of the model's dependence upon it, to be a valid and valuable technique, and have employed it previously with specific regards to “postdiction” of the top quark mass value [77]. Indeed, forcing the theoretical *output* of such a parameter is only possible in a model with highly constrained physics, and it may be expected to meet success only by intervention of either grand coincidence or grand conspiracy of Nature.

For this study, we choose a vector-like particle mass $M_V = 1000$ GeV, and use the experimental top quark mass input $m_t = 173.1$ GeV. We emphasize that the choice of $M_V = 1000$ GeV is not an arbitrary one, since a prior analysis [77] has shown that a 1 TeV vector-like mass is in compliance with all current experimental data and the No-Scale $B_\mu=0$ requirement.

In actual practice, the variation of M_{32} is achieved in the reverse by programmatic variation of the Weinberg angle, holding the strong and electromagnetic couplings at their physically measured values. Figure 9 demonstrates the scaling between $\sin^2(\theta_W)$, M_{32} (logarithmic axis), and the Z -boson mass. The variation of M_Z is attributed primarily to the motion of the electroweak couplings, the magnitude of the Higgs VEV being held essentially constant. We ensure also that the unified gauge coupling, SM fermion Yukawa couplings, and specifically also the Higgs bilinear term $\mu \simeq 460$ GeV, are each held stable at the scale M_F to correctly mimic the previously described procedure.

The parameter ranges for the variation depicted in Figure 9 are $M_Z = 91.18\text{--}92.64$, $\sin^2(\theta_W) = 0.2262\text{--}0.2357$, and $M_{32} = 1.5 \times 10^{15} \text{--} 1.04 \times 10^{16}$ GeV, and likewise also the same for Figures (10-16), which will feature subsequently. The *minimum minimorum* falls at the boundary of the prior list, dynamically fixing $M_{32} \simeq$

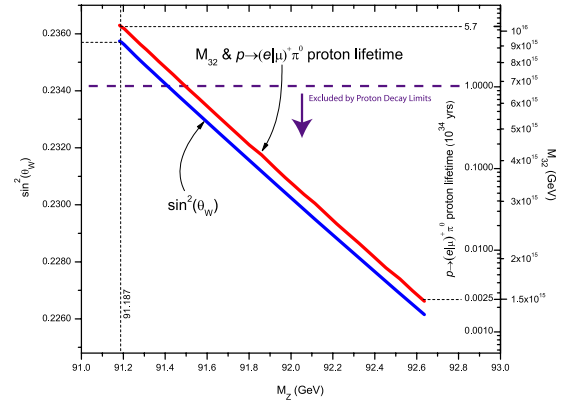


FIG. 9: The interrelated variation of $\sin^2(\theta_W)$, the GUT scale M_{32} (logarithmic axis), and the Z -boson mass M_Z is demonstrated for the parameter strips which preserve $B_\mu = 0$ and $\mu = 460$ GeV at M_F . The variation in M_Z is linked dominantly to motion of the EW couplings via $\sin^2(\theta_W)$. Also shown is the corresponding predicted proton lifetime in the leading $(e|\mu)^+\pi^0$ channels, in units of 10^{34} years, with the current lower bound of 1.0×10^{34} years indicated by the dashed horizontal purple line.

1.0×10^{16} GeV and placing $M_{1/2}$ again in the vicinity of 450 GeV. The low energy SM gauge couplings are simultaneously constrained by means of the associated Weinberg angle, with $\sin^2(\theta_W) \simeq 0.236$, in excellent agreement with experiment. The corresponding range of predicted proton lifetimes in the leading $(e|\mu)^+\pi^0$ modes is $2.5 \times 10^{31} \text{--} 5.7 \times 10^{34}$ years [49, 50]. If the GUT scale M_{32} becomes excessively light, below about 7×10^{15} GeV, then proton decay would be more rapid than allowed by the recently updated lower bound of 1.0×10^{34} years from Super-Kamiokande [81].

We are cautious against making a claim in precisely the same vein for the dynamic determination of $M_Z \simeq 91.2$ GeV, since again the crucial electroweak Higgs VEV is not a substantial element of the variation. However, in *conjunction* with the radiative electroweak symmetry breaking [82, 83] numerically implemented within the SuSpect 2.34 code base [64], the fixing of the Higgs VEV and the determination of the electroweak scale may also plausibly be considered legitimate dynamic output, *if* one posits the M_F scale input to be available *a priori*.

The present minimization, referencing $M_{1/2}$, M_{32} and $\tan\beta$, is again dependent upon M_V and m_t , while the previously described [78] determination of $\tan\beta$ was, by contrast, M_V and m_t invariant. Recognizing that a minimization with all three parameters simultaneously active is required to declare all three parameters to have been simultaneously dynamically determined, we emphasize the mutual consistency of the results. We again stress that the new *minimum minimorum* is also consistent with the previously advertised Golden Strip, satisfying all presently known experimental constraints to our available resolution. It moreover also addresses the problems of the SUSY breaking scale and gauge hierar-

chy [78], insomuch as $M_{1/2}$ is determined dynamically.

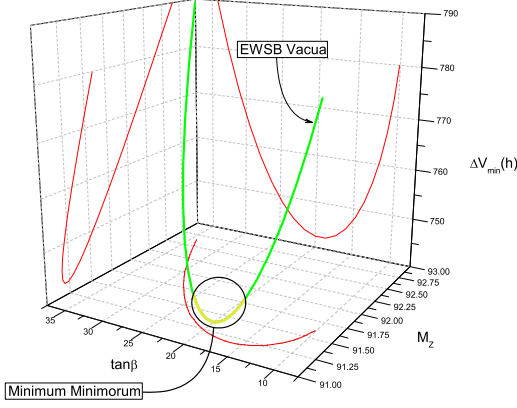


FIG. 10: Three-dimensional graph of $(M_Z, \tan \beta, \Delta V_{min}(h))$ space (green curve). The projections onto the three mutually perpendicular planes (red curves) are likewise shown. M_Z and $\Delta V_{min}(h)$ are in units of GeV. The dynamically preferred region, allowing for plausible variation, is circled and tipped in gold.

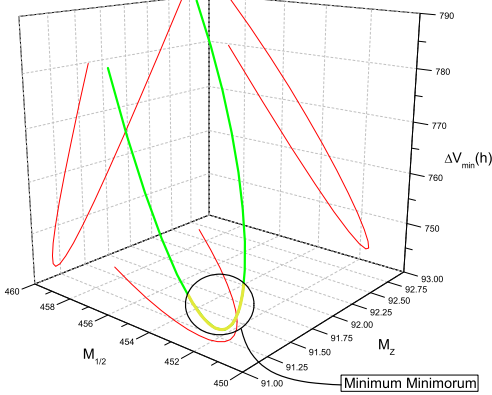


FIG. 11: Three-dimensional graph of $(M_Z, M_{1/2}, \Delta V_{min}(h))$ space (green curve). The projections onto the three mutually perpendicular planes (red curves) are likewise shown. M_Z , $M_{1/2}$, and $\Delta V_{min}(h)$ are in units of GeV. The dynamically preferred region, allowing for plausible variation, is circled and tipped in gold.

XIII. THE MINIMUM MINIMORUM OF THE HIGGS POTENTIAL: FIXING YUKAWA COUPLINGS AND μ AT $M_{\mathcal{F}}$

We have revised the `SuSpect 2.34` code base [64] to incorporate our specialized No-Scale \mathcal{F} - $SU(5)$ with vector-like mass algorithm, and accordingly employ two-loop RGE running for the SM gauge couplings, and one-loop RGE running for the SM fermion Yukawa couplings, μ term, and SUSY breaking soft terms. For our choice of $M_V = 1000$ GeV, $m_t = 173.1$ GeV, and $\mu(M_{\mathcal{F}}) \simeq 460$

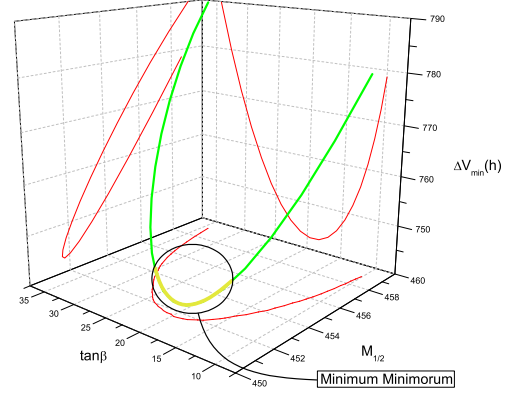


FIG. 12: Three-dimensional graph of $(M_{1/2}, \tan \beta, \Delta V_{min}(h))$ space (green curve). The projections onto the three mutually perpendicular planes (red curves) are likewise shown. $M_{1/2}$ and $\Delta V_{min}(h)$ are in units of GeV. The dynamically preferred region, allowing for plausible variation, is circled and tipped in gold.

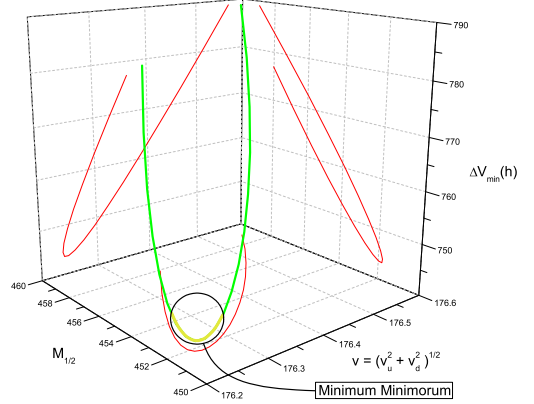


FIG. 13: Three-dimensional graph of $(v, M_{1/2}, \Delta V_{min}(h))$ space (green curve). The projections onto the three mutually perpendicular planes (red curves) are likewise shown. $M_{1/2}$, v , and $\Delta V_{min}(h)$ are in units of GeV. The dynamically preferred region, allowing for plausible variation, is circled and tipped in gold.

GeV, we present the one-loop effective Higgs potential $\Delta V_{min}(h)$ in terms of M_Z and $\tan \beta$ in Figure 10, in terms of M_Z and $M_{1/2}$ in Figure 11, in terms of $M_{1/2}$ and $\tan \beta$ in Figure 12, and in terms of v and $M_{1/2}$ in Figure 13, where $v = \sqrt{v_u^2 + v_d^2}$, $v_u = \langle H_u^0 \rangle$, and $v_d = \langle H_d^0 \rangle$. These figures clearly demonstrate the localization of the *minimum minimorum* of the Higgs potential, corroborating the dynamical determination of $\tan \beta \simeq 15 - 20$ and $M_{1/2} \simeq 450$ GeV in [78].

Additionally, we exhibit the $(M_Z, M_{1/2}, M_{32})$ space in Figure 14, the $(M_Z, M_{1/2}, v)$ space in Figure 15, and the $(M_Z, M_{1/2}, g)$ space in Figure 16, where $g = \sqrt{g_2^2 + g_Y^2}$. Figure 14 demonstrates that $M_{32} \simeq 1.0 \times 10^{16}$ GeV at the *minimum minimorum*, which correlates to $M_Z \simeq$

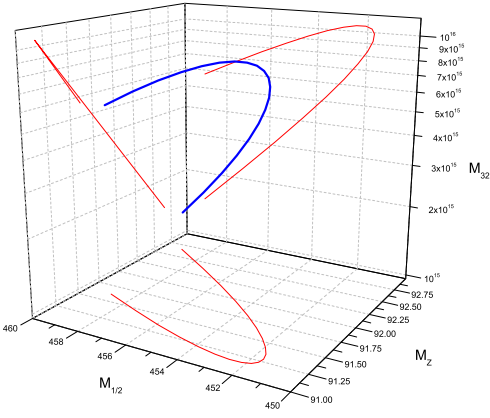


FIG. 14: Three-dimensional graph of $(M_Z, M_{1/2}, M_{32})$ space (blue curve). The projections onto the three mutually perpendicular planes (red curves) are likewise shown. M_Z , $M_{1/2}$, and M_{32} are in units of GeV.

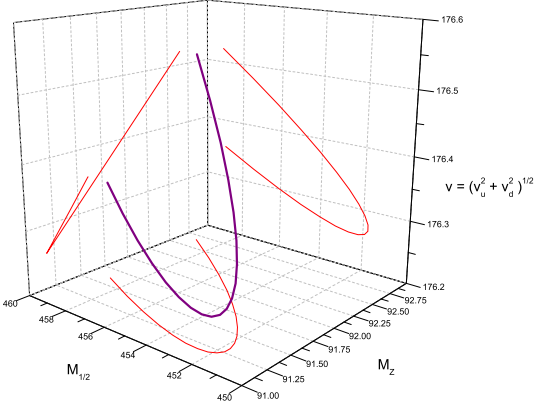


FIG. 15: Three-dimensional graph of $(M_Z, M_{1/2}, v)$ space (purple curve). The projections onto the three mutually perpendicular planes (red curves) are likewise shown. M_Z , $M_{1/2}$, and v are in units of GeV.

91.2 GeV, or more directly, $\sin^2(\theta_W) \simeq 0.236$. Together, the alternate perspectives of Figures 14, 15, and 16 complete the view given in Figures 10, 11, 12, and 13 to visually tell the story of the dynamic interrelation between the M_Z , $M_{1/2}$, and M_{32} scales, as well as the electroweak gauge couplings, and the Higgs VEVs. The curves in each of these figures represent only those points that satisfy the $B_\mu = 0$ requirement, as dictated by No-Scale supergravity, serving as a crucial constraint on the dynamically determined parameter space. Ultimately, it is the significance of the $B_\mu = 0$ requirement that separates the No-Scale \mathcal{F} - $SU(5)$ with vector-like particles from the entire compilation of prospective string theory derived models. By means of the $B_\mu = 0$ vehicle, No-Scale \mathcal{F} - $SU(5)$ has surmounted the paramount challenge of phenomenology, that of dynamically determining the electroweak scale, the scale of fundamental prominence in particle physics.

We wish to note that recent progress has been made in incorporating more precise numerical calculations into

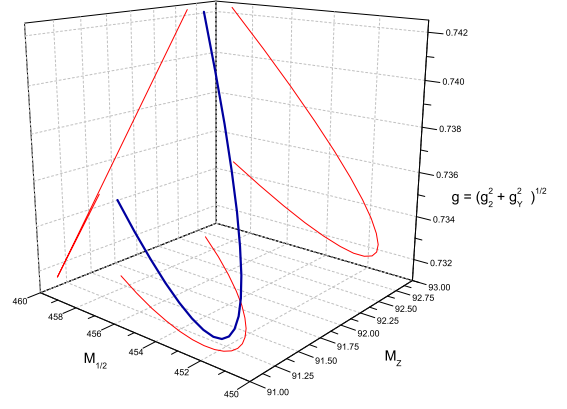


FIG. 16: Three-dimensional graph of $(M_Z, M_{1/2}, g)$ space (royal blue curve). The projections onto the three mutually perpendicular planes (red curves) are likewise shown. M_Z and $M_{1/2}$ are in units of GeV.

our baseline algorithm for No-Scale \mathcal{F} - $SU(5)$ with vector-like particles. Initially, when we commenced the task of fully developing the phenomenology of this model, the extreme complexity of properly numerically implementing No-Scale \mathcal{F} - $SU(5)$ with vector-like particles compelled a gradual strategy for construction and persistent enhancement of the algorithm. Preliminary findings of a precision improved algorithm indicate that compliance with the 7-year WMAP relic density constraints requires a slight upward shift to $\tan\beta \simeq 19 - 20$ from the value computed in Ref. [63], suggesting a potential convergence to even finer resolution of the dynamical determination of $\tan\beta$ given by the Super No-Scale mechanism, and the value demanded by the experimental relic density measurements. We shall furnish a comprehensive analysis of the precision improved algorithm at a later date.

XIV. PROBING THE BLUEPRINTS OF THE NO-SCALE MULTIVERSE AT THE COLLIDERS

We offer here a brief summary of direct collider, detector, and telescope level tests which may probe the blueprints of the No-Scale Multiverse which we have laid out. As to the deep question of whether the ensemble be literal in manifestation, or merely the conceptual superset of unrealized possibilities of a single island Universe, we pretend no definitive answer. However, we have argued that the emergence *ex nihilo* of seedling universes which fuel an eternal chaotic inflation scenario is particularly plausible, and even natural, within No-Scale Supergravity, and our goal of probing the specific features of our own Universe which might implicate its origins in this construction are immediately realizable and practicable.

The unified gaugino $M_{1/2}$ at the unification scale $M_{\mathcal{F}}$ can be reconstructed from impending LHC events by determining the gauginos M_1 , M_2 , and M_3 at the electroweak scale, which will in turn require knowledge of

the masses for the neutralinos, charginos, and the gluino. Likewise, $\tan\beta$ can be ascertained in principle from a distinctive experimental observable, as was accomplished for mSUGRA in [84]. We will not undertake a comprehensive analysis here of the reconstruction of $M_{1/2}$ and $\tan\beta$, but will offer for now a cursory examination of typical events expected at the LHC. We will present a detailed compilation of the experimental observables necessary for validation of the No-Scale \mathcal{F} - $SU(5)$ at the LHC in the following section.

For the benchmark SUSY spectrum presented in Table III, we have adopted the specific values $M_{1/2} = 453$, $\tan\beta = 15$ and $M_Z = 91.187$. We expect that higher order corrections will shift the precise location of the *minimum minimorum* a little bit, for example, within the encircled gold-tipped regions of the diagrams in the prior section. We have selected a ratio for $\tan\beta$ at the lower end of this range for consistency with our previous study [78], and to avoid stau dark matter.

TABLE III: Spectrum (in GeV) for the benchmark point. Here, $M_{1/2} = 453$ GeV, $M_V = 1000$ GeV, $m_t = 173.1$ GeV, $M_Z = 91.187$ GeV, $\mu(M_{\mathcal{F}}) = 460.3$ GeV, $\Delta V_{min}(h) = 748$ GeV, $\Omega_\chi = 0.113$, $\sigma_{SI} = 2 \times 10^{-10}$ pb, and $\langle\sigma v\rangle_{\gamma\gamma} = 1.8 \times 10^{-28}$ cm^3/s . The central prediction for the $p \rightarrow (e|\mu)^+\pi^0$ proton lifetime is around 4.9×10^{34} years. The lightest neutralino is 99.8% Bino.

$\tilde{\chi}_1^0$	94	$\tilde{\chi}_1^\pm$	184	\tilde{e}_R	150	\tilde{t}_1	486	\tilde{u}_R	947	m_h	120.1
$\tilde{\chi}_2^0$	184	$\tilde{\chi}_2^\pm$	822	\tilde{e}_L	504	\tilde{t}_2	906	\tilde{u}_L	1032	$m_{A,H}$	916
$\tilde{\chi}_3^0$	817	$\tilde{\nu}_{e/\mu}$	498	$\tilde{\tau}_1$	104	\tilde{b}_1	855	\tilde{d}_R	988	m_{H^\pm}	921
$\tilde{\chi}_4^0$	821	$\tilde{\nu}_\tau$	491	$\tilde{\tau}_2$	499	\tilde{b}_2	963	\tilde{d}_L	1035	\tilde{g}	617

At the benchmark point, we calculate $\Omega_\chi = 0.113$ for the cold dark matter relic density. The phenomenology is moreover consistent with the LEP limit on the lightest CP-even Higgs boson mass, $m_h \geq 114$ GeV [72, 73], the CDMS II [74] and Xenon 100 [75] upper limits on the spin-independent cross section σ_{SI} , and the Fermi-LAT space telescope constraints [76] on the photon-photon annihilation cross section $\langle\sigma v\rangle_{\gamma\gamma}$. The differential cross-sections and branching ratios have been calculated with PGS4 [85] executing a call to PYTHIA 6.411 [86], using our specialized No-Scale algorithm integrated into the SuSpect 2.34 code for initial computation of the particle masses.

The benchmark point resides in the region of the experimentally allowed parameter space that generates the relic density through stau-neutralino coannihilation. Hence, the five lightest particles for this benchmark point are $\tilde{\chi}_1^0 < \tilde{\tau}_1^\pm < \tilde{e}_R < \tilde{\chi}_2^0 \sim \tilde{\chi}_1^\pm$. Here, the gluino is lighter than all the squarks with the exception of the lighter stop, so that all squarks will predominantly decay to a gluino and hadronic jet, with a small percentage of squarks producing a jet and either a $\tilde{\chi}_1^\pm$ or $\tilde{\chi}_2^0$. The gluinos will decay via virtual (off-shell) squarks to neutralinos or charginos plus quarks, which will further cascade in their decay. The result is a low-energy

tau through the processes $\tilde{\chi}_2^0 \rightarrow \tilde{\tau}_1^\mp \tau^\pm \rightarrow \tau^\mp \tau^\pm \tilde{\chi}_1^0$ and $\tilde{\chi}_1^\pm \rightarrow \tilde{\tau}_1^\pm \nu_\tau \rightarrow \tau^\pm \nu_\tau \tilde{\chi}_1^0$.

The LHC final states of low-energy tau in the \mathcal{F} - $SU(5)$ stau-neutralino coannihilation region are similar to those same low-energy LHC final states in mSUGRA, however, in the stau-neutralino coannihilation region of mSUGRA, the gluino is typically heavier than the squarks. The LHC final low-energy tau states in the stau-neutralino coannihilation regions of \mathcal{F} - $SU(5)$ and mSUGRA will thus differ in that in \mathcal{F} - $SU(5)$, the low-energy tau states will result largely from neutralinos and charginos produced by gluinos, as opposed to the low-energy tau states in mSUGRA resulting primarily from neutralinos and charginos produced from squarks.

Also notably, the TeV-scale vector-like multiplets are well targeted for observation by the LHC. We have argued [77] that the eminently feasible near-term detectability of these hypothetical fields in collider experiments, coupled with the distinctive flipped charge assignments within the multiplet structure, represents a smoking gun signature for Flipped $SU(5)$, and have thus coined the term *flippons* to collectively describe them. Immediately, our curiosity is piqued by the recent announcement [87] of the DØ collaboration that vector-like quarks have been excluded up to a bound of 693 GeV, corresponding to the immediate lower edge of our anticipated range for their discovery [77].

XV. THE ULTRA-HIGH JET SIGNAL OF NO-SCALE \mathcal{F} - $SU(5)$ AT THE $\sqrt{s} = 7$ TEV LHC

The Large Hadron Collider (LHC) at CERN has been accumulating data from $\sqrt{s} = 7$ TeV proton-proton collisions since March 2010. It is expected to reach an integrated luminosity of 1 fb^{-1} by the end of 2011, all in search of new physics beyond the SM. SUSY, which provides a natural solution to the gauge hierarchy problem, is the most promising extension of the SM. Data corresponding to a limited 35 pb^{-1} has already established new constraints on the viable parameter space [88–90] due to the unprecedented center of mass collision energy. The search strategy for SUSY signals in early LHC data has been actively and eagerly studied by quite a few groups [91–95], with particular focus on the parameter space featuring a traditional mass relationship between squarks and the gluino, such as a gluino heavier than all squarks or a gluino lighter than all squarks.

A question of great interest is whether there exist SUSY models which are well motivated by a fundamental theory such as string theory, which can be tested in the initial LHC run, permitting a probe of the UV physics close to the Planck scale. In this Section we present such a model. It is well known that the supersymmetric flipped $SU(5) \times U(1)_X$ models can solve the doublet-triplet splitting problem elegantly via the missing partner mechanism [40–42]. To realize the string scale gauge coupling unification, two of us (TL and DVN) with Jiang

proposed the testable flipped $SU(5) \times U(1)_X$ models with TeV-scale vector-like particles [46], where such models can be realized in the \mathcal{F} -free \mathcal{F} -ermionic string constructions [43] and \mathcal{F} -theory model building [44, 45], dubbed \mathcal{F} - $SU(5)$. In particular, we find the generic phenomenological consequences are quite interesting [44, 45, 51].

In the simplest No-Scale supergravity, all the SUSY breaking soft terms arise from a single parameter $M_{1/2}$. The spectra in the entire Golden Strip are therefore very similar up to a small rescaling on $M_{1/2}$, with equivalent sparticle branching ratios. This leaves invariant most of the “internal” physical properties, whereas this rescaling ability on $M_{1/2}$ is not apparent in alternative SUSY models. For our analysis here, we use a vector-like particle mass of $M_V \sim 1000$ GeV, which exists in the viable parameter space; We emphasize that this is not an arbitrary choice [77], though these vector-like particles could be too heavy for observation in the early LHC run. The gluino mass is about 550 GeV, which should by contrast allow for direct testing of No-Scale \mathcal{F} - $SU(5)$ at the early LHC run.

To represent our model for this phase of analysis, we select the No-Scale \mathcal{F} - $SU(5)$ benchmark point of Table IV. The optimized signatures presented here offer an alluring testing vehicle for the stringy origin of \mathcal{F} - $SU(5)$. This point is again representative of the entire highly constrained \mathcal{F} - $SU(5)$ viable parameter space. The SUSY breaking parameters for this point slightly differ from previous \mathcal{F} - $SU(5)$ studies [63, 77, 79] inasmuch as more precise numerical calculations have been incorporated into our baseline algorithm. The masses shift a few GeV from the spectra given in previous work, but where different, we believe this to be the more accurate representation. The branching ratios and decay modes of the spectrum in Table IV and the spectra in [63, 77, 79] are identical, so the physical properties are consistent before and after code improvements. Thus, the signatures studied here will be common to the spectra provided previously.

TABLE IV: Spectrum (in GeV) for $M_{1/2} = 410$ GeV, $M_V = 1$ TeV, $m_t = 174.2$ GeV, $\tan\beta = 19.5$. Here, $\Omega_\chi = 0.11$ and the lightest neutralino is 99.8% bino.

$\tilde{\chi}_1^0$	76	$\tilde{\chi}_1^\pm$	165	\tilde{e}_R	157	\tilde{t}_1	423	\tilde{u}_R	865	m_h	120.4
$\tilde{\chi}_2^0$	165	$\tilde{\chi}_2^\pm$	756	\tilde{e}_L	469	\tilde{t}_2	821	\tilde{u}_L	939	$m_{A,H}$	814
$\tilde{\chi}_3^0$	752	$\tilde{\nu}_{e/\mu}$	462	$\tilde{\tau}_1$	85	\tilde{b}_1	761	\tilde{d}_R	900	m_{H^\pm}	820
$\tilde{\chi}_4^0$	755	$\tilde{\nu}_\tau$	452	$\tilde{\tau}_2$	462	\tilde{b}_2	864	\tilde{d}_L	942	\tilde{g}	561

For the initial phase of generation of the low order Feynman diagrams which may link the incoming beam to the desired range of hard scattering intermediate states, we have used the program **MadGraph 4.4** [96]. These diagrams were subsequently fed into **MadEvent** [96] for appropriate kinematic scaling to yield batches of Monte Carlo simulated parton level scattering events. The cascaded fragmentation and hadronization of these events into final state showers of photons, leptons, and mixed

jets has been handled by **PYTHIA** [86], with **PGS4** [85] simulating the physical detector environment. We implement MLM matching to preclude double counting of final states, and use the CTEQ6L1 parton distribution functions to generate the SM background. All 2-body SUSY processes are simulated. The b-jet tagging algorithm in **PGS4** is adjusted to update the b-tagging efficiency to $\sim 60\%$. We veto an event if any of the following conditions are met: $p_T < 100$ GeV for the two leading jets; $p_T < 350$ GeV for all jets; pseudorapidity $|\eta| > 2$ for the leading jet; missing energy $\cancel{E}_T < 150$ GeV; isolated photon with $p_T > 25$ GeV; or isolated electron or muon with $p_T > 10$ GeV. Likewise, we discard any single jet with $|\eta| > 3$. These cuts are quite standard, but alone they are insufficient to reveal the ultra-high multiplicity jet event signature; We must also investigate the event cut on the number of jets and the p_T cut on a single jet to preserve ultra-high jet events.

The detector simulations use the spectrum for the \mathcal{F} - $SU(5)$ point in Table IV. The most significant asset of the spectrum for our analysis is the relationship between the stop, gluino, and other squarks. The distinctive mass pattern of $m_{\tilde{t}_1} < m_{\tilde{g}} < m_{\tilde{q}}$ is the smoking gun signature and possibly a unique characteristic of only \mathcal{F} - $SU(5)$. To gain a comparison of the model studied here with more standardized SUSY models, we examine the ten “Snowmass Points and Slopes” (SPS) benchmark points [97] for suitable samples. We find that none of the ten SPS benchmarks support the $m_{\tilde{t}_1} < m_{\tilde{g}} < m_{\tilde{q}}$ mass pattern. This critical element is indicative of how unique the \mathcal{F} - $SU(5)$ signal could be. Previous minimal supersymmetric SM studies focused on signals from a low-multiplicity of jets, whereas the aforementioned mass pattern is expected to show a very high-multiplicity of jets. For the SPS benchmarks, we only consider those spectra not light enough to have been excluded by the initial phase of LHC data, or those not too heavy for early LHC production. A few points satisfy these criteria, though we select only one since we anticipate the corollary points to exhibit analogous characteristics. For our analysis here, we use the SPS SP3 benchmark.

Considering the large number of hadronic jets we are examining for our signatures, there is little intrusion from SM background processes after post-processing cuts. We examine the background processes studied in [91–95, 98] and our conclusion is that only the $t\bar{t} + jets$ possesses the requisite minimum cross-section and sufficient number of jets to intrude upon the \mathcal{F} - $SU(5)$ signatures. Processes with a higher multiplicity of top quarks can generate events with a large number of jets, however, the cross-sections are sufficiently suppressed to be negligible, bearing in mind the large number of ultra-high jet events which our model will generate. The same is true for those more complicated background processes involving combinations of top quarks, jets, and one or more vector bosons, where the production counts for 1 fb^{-1} of luminosity are again sufficiently small. Furthermore, we neglect the QCD 2,3,4 jets, one or more vector bosons,

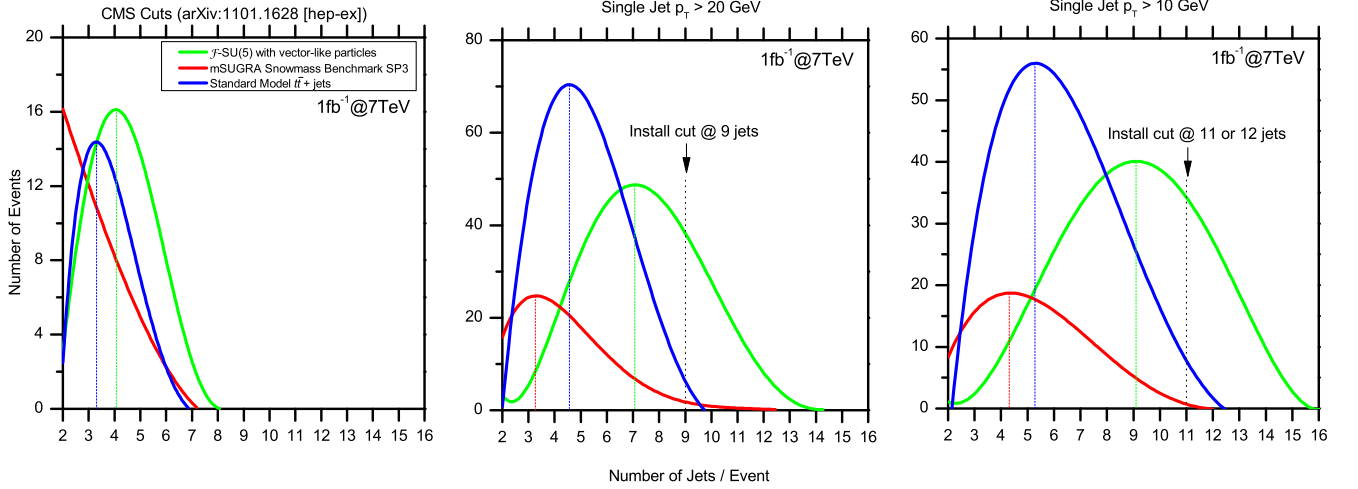


FIG. 17: Distribution of events per number of jets. For clarity of the peaks, polynomials have been fitted over the histograms.

and $b\bar{b}$ processes since none of these can sufficiently produce events with 9 or more jets after post-processing cuts have been applied.

The \mathcal{F} - $SU(5)$ with vector-like particles mass pattern produces events with a high multiplicity of virtual stops, which concludes in events with a very large number of jets through the dominant chains $\tilde{g} \rightarrow \tilde{t}_1 \bar{t} \rightarrow t \bar{t} \tilde{\chi}_1^0 \rightarrow W^+ W^- b \bar{b} \tilde{\chi}_1^0$ and $\tilde{g} \rightarrow \tilde{t}_1 \bar{t} \rightarrow b \bar{t} \tilde{\chi}_1^+ \rightarrow W^- b \bar{b} \tilde{\tau}_1^+ \nu_\tau \rightarrow W^- b \bar{b} \tau^+ \nu_\tau \tilde{\chi}_1^0$, as well as the conjugate processes $\tilde{g} \rightarrow \tilde{t}_1 t \rightarrow t \bar{t} \tilde{\chi}_1^0$ and $\tilde{g} \rightarrow \tilde{t}_1 t \rightarrow b \bar{t} \tilde{\chi}_1^-$, where the W bosons will produce mostly hadronic jets and some leptons. Additionally, the heavy squarks will produce gluinos by means of $\tilde{q} \rightarrow q \tilde{g}$. In Figure 17 we plot the number of jets per event versus the number of events for three distinct scenarios. We suppress the noise on the histogram contour to admit a more lucid distinction of the peaks in the number of jets, and fit polynomials over the data points and conceal the histograms. This allows us to gauge an appropriate selection cut for the number of jets to maximize our signal to background ratio, while assessing the impact of the selection cuts implemented by the CMS Collaboration in [88, 99]. As depicted in Figure 17, the first pane displays a comparison of the number of jets when employing the prior CMS cuts, while the remaining two panes present the results for the post-processing selection cuts defined in this paper, discriminating between two explicit cuts of the minimum p_T for a single jet. Figure 17 demonstrates that the CMS cuts of [88, 99] discard all the high-multiplicity jets, converting the events with at least 9 jets to events with few jets, thus, all information on these events with a large number of jets is lost. To retain the events with a high multiplicity of jets, we explore alternative cuts by shifting the minimum p_T for a single jet lower to the two cases of 10 GeV and 20 GeV. A minimum jet p_T of 20 GeV is secure from interfering with jet fragmentation, which typically occurs in the realm below 10 GeV, indicating that 10 GeV is

certainly fringe. We see in Figure 17 that both the 10 GeV and 20 GeV jet p_T cuts preserve the high number of jets, permitting an obvious choice for location of the cut on the minimum number of jets. We thus adopt a revised cut of single jet $p_T > 20$ GeV and total number of jets greater than 9. To assess the discovery potential, we plot the number of events per 200 GeV versus H_T , where $H_T = \sum_{i=1}^{N_{jet}} E_T^{j_i}$. Figure 18 delineates the convincing separation between the \mathcal{F} - $SU(5)$ signal and the SM $t\bar{t} + jets$ and the SP3 point. The total number of events are summarized in Table V. We also include one measure of discovery threshold that compares the number of signal events S to the number of background events B , where we require $\frac{S}{\sqrt{B}} > 5$. Notice that \mathcal{F} - $SU(5)$ comfortably surpasses this requirement.

TABLE V: Total number of events for 1 fb^{-1} and $\sqrt{s} = 7$ TeV. Minimum p_T for a single jet is $p_T > 20$ GeV.

	\mathcal{F} - $SU(5)$	SP3	$t\bar{t} + jets$
Events	93.2	2.4	10
$\frac{S}{\sqrt{B}}$	29.5	0.76	

The spectrum of Table IV exceeds the LEP constraints on the lightest neutralino $\tilde{\chi}_1^0$ and lightest stau $\tilde{\tau}_1$, and even more tantalizing, the close proximity of the stau mass beyond the LEP reach suggests imminent discovery at LHC. The stau presence can be reconstructed, for instance, from the dominant \mathcal{F} - $SU(5)$ process $\tilde{g} \rightarrow \tilde{t}_1 \bar{t} \rightarrow b \bar{t} \tilde{\chi}_1^+ \rightarrow W^- b \bar{b} \tilde{\tau}_1^+ \nu_\tau \rightarrow W^- b \bar{b} \tau^+ \nu_\tau \tilde{\chi}_1^0$. The inference of the short-lived stau in the \mathcal{F} - $SU(5)$ SUSY breaking scenario from tau production assumes fruition of the expected much improved tau detection efficiency at LHC.

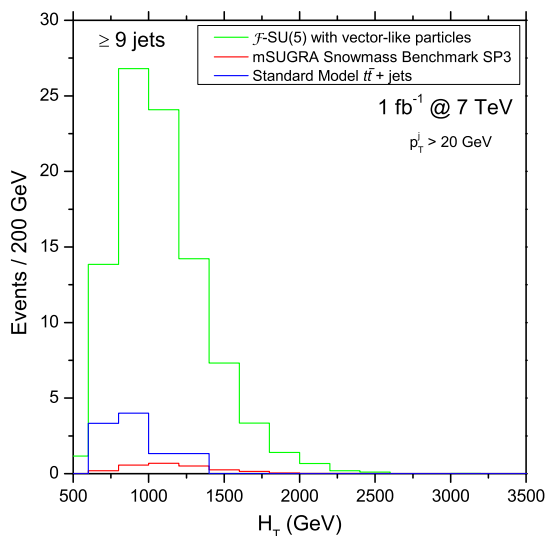


FIG. 18: Counts for events with ≥ 9 jets.

XVI. CONCLUSION

The advancement of human scientific knowledge and technology is replete with instances of science fiction transitioning to scientific theory and eventually scientific fact. The conceptual notion of a “Multiverse” has long fascinated the human imagination, though this speculation has been largely devoid of a substantive underpinning in physical theory. The modern perspective presented here offers a tangible foundation upon which legitimate discussion and theoretical advancement of the Multiverse may commence, including the prescription of specific experimental tests which could either falsify or enhance the viability of our proposal. Our perspective diverges from the common appeals to statistics and the anthropic principle, suggesting instead that we may seek to establish the character of the master theory, of which our Universe is an isolated vacuum condensation, based on specific observed properties of our own physics which might be reasonably inferred to represent invariant common characteristics of all possible universes. We have focused on the discovery of a model universe consonant with our observable phenomenology, presenting it as confirmation of a non-zero probability of our own Universe transpiring within the larger String Landscape.

The archetype model universe which we advance in this work implicates No-Scale supergravity as the ubiquitous supporting structure which pervades the vacua of the Multiverse, being the crucial ingredient in the emanation of a cosmologically flat universe from the quantum “nothingness”. In particular, the model dubbed No-Scale \mathcal{F} - $SU(5)$ has demonstrated remarkable consistency between parameters determined dynamically (the top-down approach) and parameters determined through the application of current experimental constraints (the bottom-up approach). This enticing convergence of the-

ory with experiment elevates No-Scale \mathcal{F} - $SU(5)$, in our estimation, to a position as the current leading GUT candidate. The longer term viability of this suggestion is likely to be greatly clarified in the next few years, based upon the wealth of forthcoming experimental data.

We have presented a highly constrained “Golden Point” located near $M_{1/2} = 455$ GeV and $\tan\beta = 15$ in the $\tan\beta - M_{1/2}$ plane, and a highly non-trivial “Golden Strip” with $\tan\beta \simeq 15$, $m_t = 173.0$ - 174.4 GeV, $M_{1/2} = 455$ - 481 GeV, and $M_V = 691$ - 1020 GeV, which simultaneously satisfies all the known experimental constraints, featuring moreover an imminently observable proton decay rate. In addition, we have studied the one-loop effective Higgs potential, and considered the “Super-No-Scale” condition. With a fixed Z -boson mass, we dynamically determined $\tan\beta$ and $M_{1/2}$ at the local *minimum minimorum* of the Higgs potential, while simultaneously indirectly determining the electroweak scale, thus suggesting a complete resolution of the gauge hierarchy problem in the Standard Model (SM). Furthermore, fixing the SM fermion Yukawa couplings and μ term at the $SU(5) \times U(1)_X$ unification scale, we dynamically determine the ratio $\tan\beta \simeq 15 - 20$, the universal gaugino boundary mass $M_{1/2} \simeq 450$ GeV, and consequently also the total magnitude of the GUT-scale Higgs VEVs, while constraining the low energy SM gauge couplings. In particular, these local *minima minimorum* lie within the previously described “Golden Strip”, satisfying all current experimental constraints.

The LHC era has long been anticipated for the expected revelations of physics beyond the Standard Model, as the quest for experimental evidence and insight into the structure of the underlying theory at high energies is enticingly close at hand. Consequently, the field of prospective supersymmetry models has grown as fingerprints of these models at LHC are studied. Nevertheless, our exploration of recently published signatures for supersymmetry discovery reveals a common focus toward low-multiplicity jet events. However, we showed here that manipulation of LHC data skewed toward these low jet events could mask an authentic supersymmetry signal. We have offered a clear and convincing ultra-high jet multiplicity signal for events with at least nine jets, unmistakable for the Standard Model or minimal supergravity. Notably, the optimized post-processing selection cuts outlined here are essential for discovery of supersymmetry if \mathcal{F} - $SU(5)$ is indeed proximal to the physical model. Our revised cuts are not drastic, with the two chief adjustments being lowering the minimum p_T for a single jet to 20 GeV, and raising the minimum number of jets in an event to nine. Recognition of such a signal of stringy origin at the LHC could not only reveal the flipped nature of the high-energy theory, but might also shed light on the geometry of the hidden compactified six-dimensional manifold in the string derived models, and even possibly on the hidden structure of the No-Scale Multiverse.

The blueprints which we have outlined here, integrat-

ing precision phenomenology with prevailing experimental data and a fresh interpretation of the Multiverse and the Landscape of String vacua, offer a logically connected point of view from which additional investigation may be mounted. As we anticipate the impending stream of new experimental data which is likely to be revealed in ensuing years, we look forward to serious discussion and investigation of the perspective presented in this work. Though the mind boggles to contemplate the implications of this speculation, so it must also reel at even the undisputed realities of the Universe, these acknowledged facts alone being manifestly sufficient to humble our provincial notions of longevity, extent, and largess.

The stakes could not be higher or the potential revelations more profound.

Acknowledgments

D.V.N. would like to thank Thomas Elze for his kind invitation to DICE 2010. This research was supported in part by the DOE grant DE-FG03-95-Er-40917 (TL and DVN), by the Natural Science Foundation of China under grant numbers 10821504 and 11075194 (TL), and by the Mitchell-Heep Chair in High Energy Physics (JM).

-
- [1] R. Bousso and J. Polchinski, “Quantization of four-form fluxes and dynamical neutralization of the cosmological constant,” *JHEP* **06**, 006 (2000), hep-th/0004134.
 - [2] S. B. Giddings, S. Kachru, and J. Polchinski, “Hierarchies from fluxes in string compactifications,” *Phys.Rev.* **D66**, 106006 (2002), hep-th/0105097.
 - [3] S. Kachru, R. Kallosh, A. D. Linde, and S. P. Trivedi, “De Sitter vacua in string theory,” *Phys.Rev.* **D68**, 046005 (2003), hep-th/0301240.
 - [4] L. Susskind, “The Anthropic landscape of string theory,” (2003), hep-th/0302219.
 - [5] F. Denef and M. R. Douglas, “Distributions of flux vacua,” *JHEP* **0405**, 072 (2004), hep-th/0404116.
 - [6] F. Denef and M. R. Douglas, “Distributions of nonsupersymmetric flux vacua,” *JHEP* **0503**, 061 (2005), hep-th/0411183.
 - [7] F. Denef, M. R. Douglas, and B. Florea, “Building a better racetrack,” *JHEP* **0406**, 034 (2004), hep-th/0404257.
 - [8] F. Denef, M. R. Douglas, and S. Kachru, “Physics of String Flux Compactifications,” *Ann.Rev.Nucl.Part.Sci.* **57**, 119 (2007), hep-th/0701050.
 - [9] S. Weinberg, “Anthropic Bound on the Cosmological Constant,” *Phys.Rev.Lett.* **59**, 2607 (1987).
 - [10] A. H. Guth, “The Inflationary Universe: A Possible Solution to the Horizon and Flatness Problems,” *Phys.Rev.* **D23**, 347 (1981).
 - [11] A. D. Linde, “A New Inflationary Universe Scenario: A Possible Solution of the Horizon, Flatness, Homogeneity, Isotropy and Primordial Monopole Problems,” *Phys.Lett.* **B108**, 389 (1982).
 - [12] A. Albrecht and P. J. Steinhardt, “Cosmology for Grand Unified Theories with Radiatively Induced Symmetry Breaking,” *Phys.Rev.Lett.* **48**, 1220 (1982).
 - [13] J. R. Ellis, D. V. Nanopoulos, K. A. Olive, and K. Tamvakis, “PRIMORDIAL SUPERSYMMETRIC INFLATION,” *Nucl.Phys.* **B221**, 524 (1983).
 - [14] D. V. Nanopoulos, K. A. Olive, M. Srednicki, and K. Tamvakis, “Primordial Inflation in Simple Supergravity,” *Phys.Lett.* **B123**, 41 (1983).
 - [15] D. Spergel et al. (WMAP Collaboration), “First year Wilkinson Microwave Anisotropy Probe (WMAP) observations: Determination of cosmological parameters,” *Astrophys.J.Suppl.* **148**, 175 (2003), astro-ph/0302209.
 - [16] D. Spergel et al. (WMAP Collaboration), “Wilkinson Microwave Anisotropy Probe (WMAP) three year results: implications for cosmology,” *Astrophys.J.Suppl.* **170**, 377 (2007), astro-ph/0603449.
 - [17] E. Komatsu et al. (WMAP), “Seven-Year Wilkinson Microwave Anisotropy Probe (WMAP) Observations: Cosmological Interpretation,” (2010), 1001.4538.
 - [18] P. J. Steinhardt (Cambridge University Press, 1984), pp. 251–266.
 - [19] A. Vilenkin, “The Birth of Inflationary Universes,” *Phys.Rev.* **D27**, 2848 (1983).
 - [20] E. Witten, “String theory dynamics in various dimensions,” *Nucl.Phys.* **B443**, 85 (1995), hep-th/9503124.
 - [21] C. Vafa, “Evidence for F theory,” *Nucl.Phys.* **B469**, 403 (1996), hep-th/9602022.
 - [22] E. Cremmer, S. Ferrara, C. Kounnas, and D. V. Nanopoulos, “Naturally Vanishing Cosmological Constant in $N = 1$ Supergravity,” *Phys. Lett.* **B133**, 61 (1983).
 - [23] J. R. Ellis, A. B. Lahanas, D. V. Nanopoulos, and K. Tamvakis, “No-Scale Supersymmetric Standard Model,” *Phys. Lett.* **B134**, 429 (1984).
 - [24] J. R. Ellis, C. Kounnas, and D. V. Nanopoulos, “Phenomenological $SU(1,1)$ Supergravity,” *Nucl. Phys.* **B241**, 406 (1984).
 - [25] J. R. Ellis, C. Kounnas, and D. V. Nanopoulos, “No Scale Supersymmetric Guts,” *Nucl. Phys.* **B247**, 373 (1984).
 - [26] A. B. Lahanas and D. V. Nanopoulos, “The Road to No Scale Supergravity,” *Phys. Rept.* **145**, 1 (1987).
 - [27] G. Giudice and R. Rattazzi, “Theories with gauge mediated supersymmetry breaking,” *Phys.Rept.* **322**, 419 (1999), hep-ph/9801271.
 - [28] E. Witten, “Dimensional Reduction of Superstring Models,” *Phys. Lett.* **B155**, 151 (1985).
 - [29] T. Li, J. L. Lopez, and D. V. Nanopoulos, “Compactifications of M-theory and their phenomenological consequences,” *Phys. Rev.* **D56**, 2602 (1997), hep-ph/9704247.
 - [30] C. Beasley, J. J. Heckman, and C. Vafa, “GUTs and Exceptional Branes in F-theory - I,” *JHEP* **01**, 058 (2009), 0802.3391.
 - [31] C. Beasley, J. J. Heckman, and C. Vafa, “GUTs and Exceptional Branes in F-theory - II: Experimental Predictions,” *JHEP* **01**, 059 (2009), 0806.0102.
 - [32] R. Donagi and M. Wijnholt, “Model Building with F-Theory,” (2008), 0802.2969.
 - [33] R. Donagi and M. Wijnholt, “Breaking GUT Groups in F-Theory,” (2008), 0808.2223.

- [34] M. Cvetič, T. Li, and T. Liu, “Supersymmetric Pati-Salam models from intersecting D6-branes: A Road to the standard model,” Nucl.Phys. **B698**, 163 (2004), hep-th/0403061.
- [35] C.-M. Chen, T. Li, V. Mayes, and D. V. Nanopoulos, “A Realistic world from intersecting D6-branes,” Phys.Lett. **B665**, 267 (2008), hep-th/0703280.
- [36] C.-M. Chen, T. Li, V. Mayes, and D. Nanopoulos, “Towards realistic supersymmetric spectra and Yukawa textures from intersecting branes,” Phys.Rev. **D77**, 125023 (2008), 0711.0396.
- [37] S. M. Barr, “A New Symmetry Breaking Pattern for $SO(10)$ and Proton Decay,” Phys. Lett. **B112**, 219 (1982).
- [38] J. P. Derendinger, J. E. Kim, and D. V. Nanopoulos, “Anti- $SU(5)$,” Phys. Lett. **B139**, 170 (1984).
- [39] I. Antoniadis, J. R. Ellis, J. S. Hagelin, and D. V. Nanopoulos, “Supersymmetric Flipped $SU(5)$ Revitalized,” Phys. Lett. **B194**, 231 (1987).
- [40] I. Antoniadis, J. R. Ellis, J. Hagelin, and D. V. Nanopoulos, “GUT Model Building with Fermionic Four-Dimensional Strings,” Phys.Lett. **B205**, 459 (1988).
- [41] I. Antoniadis, J. R. Ellis, J. S. Hagelin, and D. V. Nanopoulos, “An Improved $SU(5) \times U(1)$ Model from Four-Dimensional String,” Phys.Lett. **B208**, 209 (1988).
- [42] I. Antoniadis, J. R. Ellis, J. Hagelin, and D. V. Nanopoulos, “The Flipped $SU(5) \times U(1)$ String Model Revamped,” Phys.Lett. **B231**, 65 (1989).
- [43] J. L. Lopez, D. V. Nanopoulos, and K.-j. Yuan, “The Search for a realistic flipped $SU(5)$ string model,” Nucl. Phys. **B399**, 654 (1993), hep-th/9203025.
- [44] J. Jiang, T. Li, D. V. Nanopoulos, and D. Xie, “F- $SU(5)$,” Phys. Lett. **B677**, 322 (2009).
- [45] J. Jiang, T. Li, D. V. Nanopoulos, and D. Xie, “Flipped $SU(5) \times U(1)_X$ Models from F-Theory,” Nucl. Phys. **B830**, 195 (2010), 0905.3394.
- [46] J. Jiang, T. Li, and D. V. Nanopoulos, “Testable Flipped $SU(5) \times U(1)_X$ Models,” Nucl. Phys. **B772**, 49 (2007), hep-ph/0610054.
- [47] K. Nakamura, “Hyper-Kamiokande: A next generation water Cherenkov detector,” Int. J. Mod. Phys. **A18**, 4053 (2003).
- [48] S. Raby et al., “DUSEL Theory White Paper,” (2008), 0810.4551.
- [49] T. Li, D. V. Nanopoulos, and J. W. Walker, “Elements of Fast Proton Decay,” Nucl. Phys. **B846**, 43 (2011), 1003.2570.
- [50] T. Li, J. A. Maxin, D. V. Nanopoulos, and J. W. Walker, “Dark Matter, Proton Decay and Other Phenomenological Constraints in \mathcal{F} - $SU(5)$,” Nucl. Phys. B **in press** (2011), 1003.4186.
- [51] T. Li, D. V. Nanopoulos, and J. W. Walker, “Fast Proton Decay,” Phys. Lett. **B693**, 580 (2010), 0910.0860.
- [52] Y.-J. Huo, T. Li, C.-L. Tong, and D. V. Nanopoulos (2011), in Preparation.
- [53] B. Kyae and Q. Shafi, “Flipped $SU(5)$ predicts $\delta(T)/T$,” Phys. Lett. **B635**, 247 (2006), hep-ph/0510105.
- [54] S. Ferrara, C. Kounnas, and F. Zwirner, “Mass formulae and natural hierarchy in string effective supergravities,” Nucl. Phys. **B429**, 589 (1994), hep-th/9405188.
- [55] E. Cremmer and B. Julia, “The $SO(8)$ Supergravity,” Nucl.Phys. **B159**, 141 (1979).
- [56] H. P. Nilles, M. Olechowski, and M. Yamaguchi, “Supersymmetry breaking and soft terms in M theory,” Phys.Lett. **B415**, 24 (1997), hep-th/9707143.
- [57] H. P. Nilles, M. Olechowski, and M. Yamaguchi, “Supersymmetry breakdown at a hidden wall,” Nucl.Phys. **B530**, 43 (1998), hep-th/9801030.
- [58] A. Lukas, B. A. Ovrut, and D. Waldram, “On the four-dimensional effective action of strongly coupled heterotic string theory,” Nucl.Phys. **B532**, 43 (1998), hep-th/9710208.
- [59] A. Lukas, B. A. Ovrut, K. Stelle, and D. Waldram, “The Universe as a domain wall,” Phys.Rev. **D59**, 086001 (1999), hep-th/9803235.
- [60] T.-j. Li, “Soft terms in M theory,” Phys.Rev. **D59**, 107902 (1999), hep-ph/9804243.
- [61] K. Choi, A. Falkowski, H. P. Nilles, M. Olechowski, and S. Pokorski, “Stability of flux compactifications and the pattern of supersymmetry breaking,” JHEP **0411**, 076 (2004), hep-th/0411066.
- [62] K. Choi, A. Falkowski, H. P. Nilles, and M. Olechowski, “Soft supersymmetry breaking in KKLT flux compactification,” Nucl.Phys. **B718**, 113 (2005), hep-th/0503216.
- [63] T. Li, J. A. Maxin, D. V. Nanopoulos, and J. W. Walker, “The Golden Point of No-Scale and No-Parameter \mathcal{F} - $SU(5)$,” Phys. Rev. D **in press** (2011), 1007.5100.
- [64] A. Djouadi, J.-L. Kneur, and G. Moultaka, “SuSpect: A Fortran code for the supersymmetric and Higgs particle spectrum in the MSSM,” Comput. Phys. Commun. **176**, 426 (2007), hep-ph/0211331.
- [65] G. Belanger, F. Boudjema, A. Pukhov, and A. Semenov, “Dark matter direct detection rate in a generic model with micrOMEGAs2.1,” Comput. Phys. Commun. **180**, 747 (2009), 0803.2360.
- [66] “Combination of CDF and DØ Results on the Mass of the Top Quark,” (2009), 0903.2503.
- [67] N. E. Mavromatos and D. Nanopoulos, “The MAGIC of SSC and how it affects LHC,” AIP Conf.Proc. **1166**, 26 (2009), 0902.1507.
- [68] E. Barberio et al. (Heavy Flavor Averaging Group (HFAG)), “Averages of b -hadron properties at the end of 2006,” (2007), 0704.3575.
- [69] M. Misiak et al., “The first estimate of $\text{Br}(\bar{B} \rightarrow X_s \gamma)$ at $\mathcal{O}(\alpha_s^2)$,” Phys. Rev. Lett. **98**, 022002 (2007), hep-ph/0609232.
- [70] G. W. Bennett et al. (Muon g-2), “Measurement of the negative muon anomalous magnetic moment to 0.7-ppm,” Phys. Rev. Lett. **92**, 161802 (2004), hep-ex/0401008.
- [71] T. Aaltonen et al. (CDF), “Search for $B_s^0 \rightarrow \mu^+ \mu^-$ and $B_d^0 \rightarrow \mu^+ \mu^-$ decays with $2fb^{-1}$ of $p\bar{p}$ collisions,” Phys. Rev. Lett. **100**, 101802 (2008), 0712.1708.
- [72] R. Barate et al. (LEP Working Group for Higgs boson searches), “Search for the standard model Higgs boson at LEP,” Phys. Lett. **B565**, 61 (2003), hep-ex/0306033.
- [73] W. M. Yao et al. (Particle Data Group), “Review of particle physics,” J. Phys. **G33**, 1 (2006).
- [74] Z. Ahmed et al. (CDMS), “Search for Weakly Interacting Massive Particles with the First Five-Tower Data from the Cryogenic Dark Matter Search at the Soudan Underground Laboratory,” Phys. Rev. Lett. **102**, 011301 (2009), 0802.3530.
- [75] E. Aprile et al. (XENON100), “First Dark Matter Results from the XENON100 Experiment,” Phys. Rev. Lett. **105**, 131302 (2010), 1005.0380.
- [76] A. A. Abdo et al. (Fermi-LAT), “Constraints on Cosmo-

- logical Dark Matter Annihilation from the Fermi-LAT Isotropic Diffuse Gamma-Ray Measurement,” JCAP **1004**, 014 (2010), 1002.4415.
- [77] T. Li, J. A. Maxin, D. V. Nanopoulos, and J. W. Walker, “The Golden Strip of Correlated Top Quark, Gaugino, and Vectorlike Mass In No-Scale, No-Parameter F-SU(5),” (2010), 1009.2981.
 - [78] T. Li, J. A. Maxin, D. V. Nanopoulos, and J. W. Walker, “Super No-Scale \mathcal{F} -SU(5): Resolving the Gauge Hierarchy Problem by Dynamic Determination of $M_{1/2}$ and $\tan\beta$,” (2010), 1010.4550.
 - [79] T. Li, J. A. Maxin, D. V. Nanopoulos, and J. W. Walker, “Blueprints of the No-Scale Multiverse at the LHC,” (2011), 1101.2197.
 - [80] S. P. Martin, “Two-loop effective potential for the minimal supersymmetric standard model,” Phys. Rev. **D66**, 096001 (2002), hep-ph/0206136.
 - [81] H. Nishino et al. (Super-Kamiokande Collaboration), “Search for Proton Decay via $p \rightarrow e^+\pi_0$ and $p \rightarrow \mu^+\pi_0$ in a Large Water Cherenkov Detector,” Phys.Rev.Lett. **102**, 141801 (2009), 0903.0676.
 - [82] J. R. Ellis, D. V. Nanopoulos, and K. Tamvakis, “Grand Unification in Simple Supergravity,” Phys.Lett. **B121**, 123 (1983).
 - [83] J. R. Ellis, J. Hagelin, D. V. Nanopoulos, and K. Tamvakis, “Weak Symmetry Breaking by Radiative Corrections in Broken Supergravity,” Phys.Lett. **B125**, 275 (1983).
 - [84] R. L. Arnowitt, B. Dutta, A. Gurrola, T. Kamon, A. Krislock, et al., “Determining the Dark Matter Relic Density in the mSUGRA (X0(1))-tau Co-Annihilation Region at the LHC,” Phys.Rev.Lett. **100**, 231802 (2008), 0802.2968.
 - [85] J. Conway et al., “PGS4: Pretty Good (Detector) Simulation,” (2009), URL <http://www.physics.ucdavis.edu/~conway/research/>.
 - [86] T. Sjostrand, S. Mrenna, and P. Z. Skands, “PYTHIA 6.4 Physics and Manual,” JHEP **05**, 026 (2006), hep-ph/0603175.
 - [87] V. M. Abazov et al. (D0 Collaboration), “Search for single vector-like quarks in $p\bar{p}$ collisions at $\sqrt{s} = 1.96$ TeV,” Phys.Rev.Lett. (2010), long author list - awaiting processing, 1010.1466.
 - [88] V. Khachatryan et al. (CMS), “Search for Supersymmetry in pp Collisions at 7 TeV in Events with Jets and Missing Transverse Energy,” (2011), 1101.1628.
 - [89] J. B. G. da Costa et al. (Atlas), “Search for supersymmetry using final states with one lepton, jets, and missing transverse momentum with the ATLAS detector in $\sqrt{s} = 7$ TeV pp,” (2011), 1102.2357.
 - [90] J. B. G. da Costa et al. (Atlas), “Search for squarks and gluinos using final states with jets and missing transverse momentum with the ATLAS detector in $\sqrt{s} = 7$ TeV proton-proton collisions,” (2011), 1102.5290.
 - [91] H. Baer, V. Barger, A. Lessa, and X. Tata, “Capability of LHC to discover supersymmetry with $\sqrt{s} = 7$ TeV and 1 fb^{-1} ,” JHEP **06**, 102 (2010), 1004.3594.
 - [92] G. L. Kane, E. Kuflik, R. Lu, and L.-T. Wang, “Top Channel for Early SUSY Discovery at the LHC,” (2011), 1101.1963.
 - [93] D. Feldman, K. Freese, P. Nath, B. D. Nelson, and G. Peim, “Predictive Signatures of Supersymmetry: Measuring the Dark Matter Mass and Gluino Mass with Early LHC data,” (2011), 1102.2548.
 - [94] O. Buchmueller et al., “Implications of Initial LHC Searches for Supersymmetry,” (2011), 1102.4585.
 - [95] M. Guchait and D. Sengupta, “Searches for Supersymmetry at the LHC with 7 TeV energy,” (2011), 1102.4785.
 - [96] J. Alwall et al., “MadGraph/MadEvent v4: The New Web Generation,” JHEP **09**, 028 (2007), 0706.2334.
 - [97] B. C. Allanach et al., “The Snowmass points and slopes: Benchmarks for SUSY searches,” Eur. Phys. J. **C25**, 113 (2002), hep-ph/0202233.
 - [98] B. Altunkaynak, M. Holmes, P. Nath, B. D. Nelson, and G. Peim, “SUSY Discovery Potential and Benchmarks for Early Runs at $\sqrt{s} = 7$ TeV at the LHC,” Phys. Rev. **D82**, 115001 (2010), 1008.3423.
 - [99] “Search strategy for exclusive multi-jet events from supersymmetry at CMS,” (2009), CMS PAS SUS-09-001, URL <http://cdsweb.cern.ch/record/1194509>.